

Interactive comment on “Comparison and validation of global and regional ocean forecasting systems in the South China Sea” by X.

Zhu et al.

L. Lusito (Referee)

letizia.lusito@cmcc.it

Received and published: 31 March 2016

1. General comments

First of all, I would like to congratulate all the authors for the good scientific level of the work presented in this paper. This paper addresses the relevant problem of comparison and validation with real observations of two ocean models (SCSOFS and MO) in the South China Sea, an area which is becoming more and more strategic. Ocean models, in general, are the key to improve our knowledge of the sea state, present and future, on which to base political, environmental, economical decisions by governments and other stakeholders. In this respect, these issues are relevant not only to the general themes addressed by this journal, but also they are especially relevant in the context of this special issue subject ‘Situational sea awareness technologies for maritime safety and marine environment protection’.

The results described here can be considered innovative; in fact, even if the South China Sea Ocean Forecasting System for the regional modelling of the south China Sea, and the global Ocean model, developed by Mercator Ocean, have been described in previous works, their comparison and validation with real observations in the South China Sea is a new important result that will allow a substantial improvement of the ocean forecasting capability in the area. Moreover the paper shows how both models could be improved regarding the forecast skills in case of devastating events like typhoons which are unfortunately not rare in that region.

The title is clear and reflects the content of the paper. The abstract provides a good summary of the results and of the conclusions that derive from them in a language easily understandable by the average reader. Every section describes clearly a particular aspect of the data, model or method used. The overall length is adequate and a good compromise between a too-long discussion containing a full description of many technical details and a too short description of the results without a proper introduction of the context, methods and data used.

It is strongly recommended that the English language is revised and improved by a native speaker although the actual form is sufficiently understandable. Some suggestions to improve the text will be reported separately.

Other comments (about units, figures, references, further clarifications) are reported in the next sections.

We sincerely appreciate the reviewer for the constructive comments and suggestions. We addressed these concerns in the revision by following all the suggestions to significantly improve the manuscript in the following manner:

- 1) We have explained relative words or sentences and answered all the questions of the reviewer.
- 2) We have clarified the introductions to the satellite data, SLA, MGDSST, AVHRR in section 2.1.
- 3) We redraw or modified relative figures mentioned by the review, such as Fig. 1,2,4,5,6,7,8,10.
- 4) We revised all the styles, language, typos, references

2. Specific scientific comments

Line 17: explain or define better what you are referring to with the term "mesoscale activities"

We have explained it by adding the words “, such as ocean fronts, Typhoon, and mesoscale eddy,”

Line 74: explain better what you mean with the phrase "where they can then impact budgets of the tracers"

We have changed it to “where they can then impact budgets of heat, mass, momentum and biogeochemical properties”.

Line 107: if the satellite data you use are from 2012, what is "April 2014" referring to? The starting date of the SSALTO/DUACS new data system?

The satellite datasets, DUACS 2014 version, are distributed to users in April 2014, which including the data from 1993 to present. We only use the data of 2012 to compare and validate our systems' results in this paper.

Line 109: quoting from the user manual of the L4 altimeter data you are using (and that you cite http://www.aviso.altimetry.fr/fileadmin/documents/data/tools/hdbk_duacs.pdf) "Change of resolution: in DUACS 2014 version, after the feedback from users, the Mercator grid projection with 1/3 x1/3 spatial resolution (Global product) is abandoned. The DUACS 2014 Global products are directly computed on a Cartesian 1/4 x1/4 spatial resolution." Therefore, depending which data you are using, it may be incorrect saying that the products are sampled from the Mercator gridded data so please, specify better if you are using the DUACS 2014 data or a former version (and which one). From the following discussion it seems you are using the DUACS 2014 data.

Yes, we use the DUACS 2014 data in this paper and have modified it in the revised manuscript.

Line 115: quoting the JMA database description of the MGDSST (<http://neargoos1.jodc.go.jp/rmdb/format/JMA/mgdsst.txt>): "Merged satellite and in-situ data Global Daily Sea Surface Temperature (MGDSST): The MGDSSTs are analysed at the Office of Marine Prediction of the JMA with 1/4-degree grid resolution on the near realtime basis. SSTs derived from satellite's infrared sensors (AVHRR/NOAA) and microwave sensor (AMSR-E/AQUA), and in-situ SST (buoy and ship) are used in the analysis." The list of satellite products here does not match the list of satellite products you mention in the paper.

Thanks, we have revised it to match the description of the MGDSST in the website.

Line 122-127 please clarify in the paper that the reason for which you are using the "AVHRR-only" data is because the production of the AVHRR+AMSR data ended in 2011. Otherwise questions might arise on the impact of the usage of "AVHRR+AMSR" data in your analysis and how the results might differ from the results using "AVHRRonly" data.

Thanks, we have clarified it in the revised manuscript by adding the words “Since the production of the AVHRR+AMSR data ended in 2011” at line 145.

Line 137-138: just for my education: why to filter out the tidal signal you use a period of 25 hours and

not, for example 24 hours? Same, why did you use a 25-hour period to calculate the daily average?

It is because the periods of some of the major diurnal tidal constituents are longer than 24 hours. Actually 26 hours is better than 25 hours to filter out the tidal information.

Line 140 and following: you mention that there were 5 cruises to measure the temperature/salinity data but you use data from only two of them for the TS distribution comparison? Why only two? Why do you use the data from these particular cruises? Are the data from the remaining three cruises significantly different in some ways? What changes/improvements/impacts do you expect when using all the data available?

We did have compared both two systems with other three cruises, the results are almost the same. In order to save space, we only show two of them in this paper. The Qiongdong cruise is conducted in the coastal area, the Nansha cruise is conducted in the deep area. We also compared all the measured TS data from 5 cruises with the two system, please see Fig. 9 and section 3.2.3 Correlation ship between model and in-situ.

Line 244: be more specific than "little stronger than AVISO" For example you can add a time-series-like plot showing the basin-averaged, minimum and maximum velocities (in separated components u and v) for the two models and the satellite observations in the four months. On the x-axis you have the 4 time steps (Jan, Apr, Jul, Oct.), on the y-axis 3 u-velocities (min, max, basin-averaged) for each of the two models and the observation. Same for v. Alternatively, at least quote the basin-averaged velocities in the text. From the Figure only, it is very difficult to distinguish the length of the vectors hence to have an estimation of the magnitude of the velocities. Moreover, while on lines 243 you say that AVISO shows currents that are smaller than MO or SCSOFS, at lines 249 you say that AVISO has comparable velocities to MO and SCSOFS has smaller velocities so there is an incongruence in the text.

Thanks. It is not correct, we have deleted the words "except that the current speeds are a little stronger than AVISO".

Line 260: explain why in your opinion in spring the two models and the observation show each a different type of Kuroshio intrusion. Is this maybe due to some physics effects modelled differently in the two models or boundary conditions not implemented in the best way in the two models. Can you also explain why this effect is visible mainly in spring?

It is obviously the types of Kuroshio intrusion are different from each among the three results, you can refer the paper Nan et al. (2011a). And AVISO, MO, and SCSOFS show the leaking path, looping path, and leaping path in spring, respectively. Actually, I have not researched much on this problem. I think it is an interesting scientific problem, and additional work need to do to study it in detail. But this is out of the scope of this paper.

In my opinion, it may due to the surface wind forcing are different for the two models. Since the wind is weaker in spring than other seasons in this area, the wind forcing used in both two models may not agreement well with the real wind.

Line 271: I would prefer to use the word "temporal" instead of "phase" bias in this case. The word phase is generally more used when speaking about angles. Do you have an explanation about this temporal behaviour of SCSOFS?

Thanks, we have changed the word from "phase" to "temporal". It may due to the surface wind forcing, we will double check about it.

At line 281 you say that the SST has been assimilated in SCSOFS but this is not mentioned when you describe which data are assimilated in the model in lines 187 and 188.

Yes, the SST data has been assimilated in SCSOFS by the thermal feedback method to correct net surface

heat flux (Barnier et al., 1995). We have modified the description at Line 189 and 190.

At line 286 you say that the SST variation is larger in winter and smaller in summer for both MO and SCSOFS but when looking at Figure 4 this appears to not be true: the absolute magnitude of the variation is much larger for SCSOFS (where you see large blue and red areas) than for MO (where you see prevalent green everywhere) and has the same values (but with opposite signs) for summer and winter; in winter the area that show a large variation is simply larger so it is better to specify the basin-averaged variation is larger. What it seems more correct is that SCSOFS overestimates the SST in winter and underestimates the SST in summer, therefore has a more uniform trend of the SST through the year with respect to MO

Thanks, we have modified it at line 286.

Line 287 you quote 3 values for RMSE for each of the models saying that they are the maximum minimum mean monthly but it is no clear what do you mean with "monthly": are these the averaged values over the 4 months or do they correspond to a specific month? In any case please quote the values for each month for a better comparison of the performances of MO and SCSOFS

Thanks, we have modified it at line 298 in the revised version.

Line 303: you say that the isohaline is located at 50 km for in-situ data and SCSOFS and at 20 km for MO but this big difference is not so evident in Figure 6, therefore from Figure 6 it cannot be concluded that SCSOFS performs better than MO when compared to in-situ data. A plot of a vertical profile of TS and the TS bias for let's say 20km, 50 km and 70 km can clarify better the performances of the models in this case.

We have changed the plot of SCSOFS in Figure 6, and revised the position of MO from 20km to 40km.

Line 375 Define what is W

W is the Okubo-Weiss parameter (Xiu et al., 2010) defined as:

$$W = S_n^2 + S_s^2 - \omega^2,$$

Where

$$S_n = \frac{\partial u}{\partial x} - \frac{\partial v}{\partial y}$$

$$S_s = \frac{\partial v}{\partial x} + \frac{\partial u}{\partial y}$$

$$\omega = \frac{\partial v}{\partial x} - \frac{\partial u}{\partial y}$$

Line 387 Why do you use a period of 24 years for SCSOFS and just one year for MO?

Since we have got only the year of 2012 data from MO, only one year of MO data is available in this study, and 14 years, from 2001 to 2014 for SCSOFS.

Line 391 You say that all the three results show a small number of eddies in autumn and a larger number of eddies in spring but this is not true for MO when looking at table 1, where MO predicts 13 total eddies for both spring and autumn

Thanks, we have revised it as: "As for the seasonal distributions (figures not shown), all three data have most eddies in spring. Both AVISO and SCSOFS have less eddies in fall and more cyclones than anti-cyclones in spring and fall, and all three have less cyclones than anti-cyclones in summer."

Line 395 explain better the oversimplification of SLA calculation for MO and why SCSOFS does not suffer from this.

Oversimplification here means SLA calculated by only one year's MO data averaged and extracted from

SSH. This may introduce great error for SLA and the eddy identification.

3. Style comments and suggestions

3.1 General

Be consistent with the space between the value and the unit of measure, for example in line 28 you write "1200m" and line 156 you write "0.16 m". As a general reference, the NIST Guide for the Use of the International System of Units (SI) states "7.2 Space between numerical value and unit symbol: In the expression for the value of a quantity, the unit symbol is placed after the numerical value and a space is left between the numerical value and the unit symbol. The only exceptions to this rule are for the unit symbols for degree, minute, and second for plane angle (...) in which case no space is left between the numerical value and the unit symbol."

Thanks, we have modified all the expressions in the revised paper.

Change all the "northeastly" in "northeasterly" , "southwestly" in "southwesterly" and all the similar words.

Thanks, we have changed them in the revised paper.

Use consistently "coastal currents" or "Coastal Currents" (check for examples line 50-51)

Thanks, we have changed them in the revised paper.

Be consistent in using 1/4 or 0.25 for the horizontal resolutions (for example lines 116 and 119)

Thanks, we have changed them in the revised paper.

In the section about MO (2.4), you keep calling the model PSY4V1R3 systematically without any mention of Mercator Ocean and in the later sections this name (PSY4V1R3) disappears. Please introduce at some point in section 2.4 a clarification like : the PSY4V1R3 configuration described here is indicated for as MO model through this paper.

Thanks, we have clarified it in the revised paper.

3.2 References

Bell, 2015 is never used; Chu, 2001 is never used; Daudin, 2013 never used;

Thanks, we have deleted these references.

Weiss 1991, not used;

Thanks, we have added the citation at line 395.

Line 167: move the reference to SODA to the line where you first talk about SODA, i.e. line 91;

Thanks, we have added the citation at line 395.

Line 179: The reference for Barnier 1995 is missing. In the reference there is a Barnier 2006. Please check.

Thanks, we have added the reference for Barnier et al., 1995 at line 485.

Line 185: the reference for Wang et al 2012 is missing.

Thanks, we have added the reference for Wang et al., 2012 at line 638

Please check Line 201: move the reference to the Arakawa C-grid to where you first introduce the Arakawa C-grid, i.e. line 152.

We have moved it to line 164

Line 228 : the reference WOA2005 is missing

We have added the references Antonov et al., 2006 and Locarnini et al., 2006

3.3 Figures

In general increase the size of the x/y labels especially in the maps and use higher resolution files so that the image does not loose sharpness when zooming in.

Fig 1: change the colours for the cruises paths and the mooring station because now they cannot be

easily distinguished from the background Moreover, please indicate in Fig.1 more of the channels and seas you name in lines 30-33 to facilitate the nonexpert readers in understanding the unique geographical features of the SCS. Reduce the width (or the size in general to keep the aspect ratio) because the label of the scale is outside the printing area so it is missing in a printed version of the paper

Thanks. We have tried to change colours for the cruises paths and the mooring station to the yellow, red and others, found the pink, green and black are the best colors to distinguish from the background. We also have added the names of channels and seas, such as Karimata Strait, Balabac Strait, Mindoro Strait, Java Sea, Sulu Sea, and East China Sea, and reduced the width.

Fig.2: report in a separate plot the mean maximum and minimum AGV because it is currently difficult to compare them from the maps shown in Fig.2 or report these values explicitly in the text. Increase the sizes of the labels on the legend and axes. Use higher resolution files. The unity of measure is missing from the scale Also SSH bias maps can be added (MO minus AVISO and SCSOFS minus AVISO) to evidence better the behaviour of the two models with respect to the observations (analogous to Fig.4 maps)

Thanks. We have changed color shaded of all plots from Sea Surface Height to the speeds of AVG in Fig. 2. Since we have not mentioned Sea Surface Height in the text. And we also have increased the sizes of the labels on the legend and axes and added the unity of measure of the scale.

Maybe you can also change the color map for Figure 4: a red/white/blue (RWB) map is usually more appropriate to represent bias. For example in the actual maps the green color can correspond to bias values of both +0.5 and -0.5; using a RWB map would make more clear the areas where the bias is positive and where it is negative.

Thanks, we have changed it follow your suggestion.

Fig.5-6-7-8: units missing from the colorbar

Thanks, we have added it.

Fig.9: the correlation plots for salinity show a less good linear relationship between MO and SCSOFS and data with respect to the same plots for temperature? Did you try to plot the correlations in different depth ranges to see if the plots show a better linear correlation and if there is a depth range for which the correlation is not good and this degrades the overall linear relationship?

Yes, we have tried to plot it in different depth, and got almost the same results. So we just show the whole linear relationship in this paper. It is actually that the correlation for salinity is less than those for temperature.

Fig 10: change the colormap so that also the pale yellow structures can be distinguished better from the white background

Thanks, we have changed it follow your suggestion.

Fig.11: explain what are the white areas on the map

The white areas mean the SST increasing.

3.4 Language and typos

Line 12-13: change "Mercator Ocean...in China" in "the global Mercator Ocean Operational System , developed and maintained by Mercator Ocean in France and the regional South China Sea Operational Forecasting System (SCSOFS) by the National Marine Environmental Forecasting Center (NMEFC) in China". I think it is better to underline that MO is a global ocean forecasting system developed by Mercator Ocean, a scientific institution in France.

Line 22: change "AVISO data" in "satellite observations": at this point it is not yet clear to a medium reader what are AVISO data; change "results compared in above" in "outcome of the results comparison"

Line 42-43: change "in the NSCS...in the SSCS" in "is present in the NSCS, while a semiannual/biennial change from a cyclonic gyre regime in winter to an anti-cyclonic gyre regime in summer can be observed in the SSCS" Please note that the word "biannual" is ambiguous; some use it with the meaning of "twice per year" in which case it is better to use the word "semiannual", others use it to say "every two years", in which case it is better to say "biennial".

Line 136 change "abnormal" in "outlier"

Line 142/263: change "See" in "see"

Line 145-147: change "All the measured...correlation analysis" in "The TS data collected from all the 5 cruises will be used to perform a correlation analysis of each of the simulated predictions of MO and SCSOFS models with the observations."

Line 149: change "Ocean" in "Oceanic" and modelling in "modeling". The first correction comes from the original name of ROMS while the second is to align the spelling of the word to the American English rule that you are using in other words (for example as in "analyzed")

Line 208: the value " $-1 \times 10^{10} \text{ m}^4 \text{ s}^{-1}$ " seems odd, please check in case there is a typo.

Line 216: remove the comma before the parenthesis

Line 218 add a "-" between along and track

Line 221: since it is the first time you mention SSH add the full name: Sea Surface Height (SSH) and remove the full name from line 232

Line 267 there must be a typo in "the range of large is less than". Please rewrite. Change "leading" in "anticipating"

Line 317 change "ship" in "analysis"

Line 320 remove "of relativity"

Line 354 substitute "hot" with important

Line 367 substitute "SST deceasing" with "SST decrease"

Line 415 there is a typo: the first SCSOFS should be changed in MO

Thanks, we have changed all the typos in above in the revised paper.

Interactive comment on Nat. Hazards Earth Syst. Sci. Discuss., doi:10.5194/nhess-2016-60, 2016.

1 **Comparison and validation of global and regional ocean**
2 **forecasting systems in the South China Sea**

3 Xueming Zhu¹, Hui Wang¹, Guimei Liu^{1*}, Charly Régnier², Xiaodi Kuang¹, Dakui
4 Wang¹, Shihe Ren¹, Zhiyou Jing³, Marie Drévillon²

5
6 ¹Key Laboratory of Research on Marine Hazards Forecasting, National Marine Environmental
7 Forecasting Center, Beijing, 100081, China

8 ²Mercator Océan, Ramonville Saint Agne, France

9 ³State Key Laboratory of Tropical Oceanography, South China Sea Institute of Oceanology, Chinese
10 Academy of Sciences, Guangzhou, 510301, China

11 *Correspondence to:* Guimei Liu (liugm@nmefc.gov.cn)

12 **Abstract.** In this paper, the performances of two operational ocean forecasting systems, the global
13 Mercator Océan (MO) Operational System, developed and maintained by Mercator Océan in France and
14 the regional South China Sea Operational Forecasting System (SCSOFS) by the National Marine
15 Environmental Forecasting Center (NMEFC) in China, have been examined. Both systems can provide
16 science-based nowcast/forecast products, such as temperature, salinity, water level and ocean
17 circulations. Based on the observed satellite and *in-situ* data have been obtained in 2012 in the South
18 China Sea, the comparison and validation of the ocean circulations, the structures of the temperature and
19 salinity, and some mesoscale activities, such as ocean fronts, Typhoon, and mesoscale eddy, are shown.
20 Comparing with the observation, the ocean circulations and SST of MO show better results than those of
21 SCSOFS. However, the structures of temperature and salinity of SCSOFS are better than those of MO.
22 For the mesoscale activities, SST fronts and SST decreasing during the typhoon Tembin of SCSOFS are
23 better agreement with the previous study or satellite data than those of MO; but both of them show some
24 differences from satellite observations. Finally, according to the outcome of the results comparison,
25 some suggestions have been proposed for both systems to improve their performances in the near
26 further.

27 **Keywords.** SCSOFS, Mercator Océan, South China Sea, Operational Forecasting System

28 1 Introduction

29 The South China Sea (SCS, Fig.1) is the largest and deepest semi-enclosed marginal sea of the
30 Northwestern Pacific (NWP), with the area is about 3.5 million km², the mean and maximum depth is
31 about 1200_m and 5300_m, respectively. A wide continental shelf with depth less than 200_m located in
32 the northern SCS (NSCS). There are numerous islands, reefs, beaches, shoals in large basin of the
33 southern SCS (SSCS). It is connected with the adjacent seas through a number of channels, to the East
34 China Sea in north, the NWP in east, the Sulu Sea in southeast, and the Java Sea in south, by the Taiwan
35 Strait (TWS), the Luzon Strait (LUS), the Mindoro Strait and the Balabac Strait, the Karimata Strait,
36 respectively. Its unique geographical features, rich marine mineral and petroleum resources play a
37 significant role to many countries adjacent to it.

38 The SCS is located in the East Asian Monsoon (EAM) winds regime, the northeasterly winds usually
39 prevail with an average wind speed of 9_m/s over the whole domain in winter, while the southwesterly

删除的内容: AVISO data

删除的内容: ed in above

42 winds prevail with an average magnitude of 6m/s dominating over the most parts of the SCS in summer
43 (Hellerman and Rosenstein, 1983). The EAM is considered to be the main factor for driving the upper
44 layer basin-scale circulation pattern in the entire SCS, showing an obvious seasonal variation with a
45 cyclonic gyre in winter and an anti-cyclonic gyre in summer (Wyrki, 1961; Mao et al., 1999; Wu et al.,
46 1999; Qu, 2000; Chu and Li, 2000). However, some other literatures insist that a persistent cyclonic gyre
47 is present in the NSCS, while a semiannual change from a cyclonic gyre in winter to an anti-cyclonic
48 gyre regime in summer can be observed in the SCS (Chao et al., 1996; Takano et al., 1998; Hu et al.,
49 2000; Chern and Wang, 2003; Caruso et al., 2006; Chern et al., 2010). Chern et al. (2010) suggested that
50 the three dynamical processes, the wind stress curl, the deep-water ventilation-induced vortex stretching
51 in the central SCS, and a positive vorticity generated from the left flank of the Kuroshio in the LUS, play
52 the equal importance to the formation of the persistent cyclonic gyre in the NSCS, according to the
53 analysis of the results from several numerical experiments with different wind stress, topography and
54 coastline.

55 In addition to the basin-scale circulations, there are still some sub-basin scale currents in the SCS, such as
56 the Guangdong Coastal Current (Huang et al., 1992), the SCS Warm Current (SCSWC, Guan, 1978;
57 Chao et al., 1995), Dongsha Coastal Current (DCC, Su, 2005), Luzon Coastal Current (LCC, Hu et al.,
58 2000), and so on. However, there are still a lot of debates about the mechanisms of some of them among
59 the studies reported by several authors, without reaching an agreement. For example, based on the results
60 of the numerical simulations, the formation dynamical mechanism of the SCSWC may be related to the
61 Kuroshio intrusion (Li et al., 1993; Cai and Wang, 1997), sea surface slope (Fang and Zhao, 1988; Guan,
62 1993), or the wind relaxation (Chao et al., 1995).

63 The Kuroshio intrudes into the SCS through the LUS, carrying the warm and salty water from the NWP,
64 significantly affecting the circulation pattern and the budgets of heat and salt in the NSCS (Farris and
65 Wimbush, 1996; Wu and Chiang, 2007; Liang et al., 2008; Nan et al., 2013). However, it is still not in
66 accordance with how the Kuroshio intrudes into the NSCS. As pointed out in Hu et al. (2000), there
67 existed four viewpoints on the Kuroshio intrusion as, a direct branch from the Kuroshio (Williamson,
68 1970; Fang et al., 1996; Chern and Wang, 1998; Qu et al., 2000), a form of loop (Zhang et al., 1995; Liu
69 et al., 1996; Farris and Wimbush, 1996), a form of extension (Hu et al., 1999), and a form of ring (Li et al.,
70 1998a, b) at present. Nan et al. (2015) reviewed and summarized the Kuroshio intruding processes from
71 observed data, numerical experiments and theoretical analyses, and concluded that there were three

删除的内容: bi

删除的内容: ly

删除的内容: ing

删除的内容: c

删除的内容: c

77 typical paths of the Kuroshio intruding the SCS, the looping path, the leaking path and the leaping path,
78 which could be distinguished quantitatively by a Kuroshio SCS Index (KSI, Nan et al., 2011a) derived
79 from the integral of geostrophic vorticity southwest of Taiwan. The three paths can change from one to
80 another in several weeks.

81 In addition, many mesoscale eddy activities are another obvious physical characteristics of the NSCS,
82 and play a great influence on the dynamical environment of the NSCS. Eddies are generally more
83 energetic than the surrounding currents and are an important component of dynamical oceanography at
84 all scales. In particular they transport heat, mass, momentum and biogeochemical properties from their
85 regions of formation to remote areas where they can then impact budgets of heat, mass, momentum and
86 biogeochemical properties. Eddies in the NSCS have attracted increasing attention over recent a few
87 decades. Much work has been done based on the combination of satellite observation and *in-situ*
88 hydrographic data (Wang and Chern, 1987; Li et al., 1998; Chu et al., 1999; Wang et al., 2003; Hu et al.,
89 2011; Nan et al., 2011b), or numerical models (Wu and Chiang, 2007; Xiu et al., 2010; Zhuang et al.,
90 2010). Some of work has been focused on the statistical characteristics of eddies in the SCS, but they are
91 greatly different from each other, owing to different criteria for eddy identification employed by different
92 literatures (Wang et al., 2003; Xiu et al., 2010; Du et al., 2014). Some of work analyzes eddies' seasonal
93 variability (Wu and Chiang, 2007; Zhuang et al., 2010) and investigates their genesis (Wang et al., 2008).
94 Some of work mainly studies specific eddies to better understand eddy's generation, development and
95 disappearance mechanisms (Wang et al., 2008; Zhang et al., 2013).

96 As shown above, the dynamic processes and relative mechanisms are very complex, but still not cleared
97 until now in the SCS. It will be much more difficult to predict the status of the future ocean. National
98 Marine Environmental Forecasting Center (NMEFC) is mainly responsible for the prediction of the sea
99 area of the South China Sea, has built a SCS Operational Forecasting System (SCSOFS). As is known to
100 all, the open boundary forcing plays an important role in the numerical prediction of the regional ocean.
101 Due to the various limitations, the current SCSOFS' open boundary conditions (OBC) are derived from
102 the Simple Ocean Data Assimilation (SODA, Carton and Giese, 2008) climatological monthly mean
103 during the forecast run. It is extremely inappropriate for the real-time ocean prediction system, so we
104 plan to transform the OBC from SODA to the real-time forecasting results derived from Mercator Océan
105 (MO) on the next step, in order to further improve prediction accuracy of the SCSOFS. Before carrying
106 out this work, it is necessary to compare and validate the performance of MO in the SCS.

删除的内容: the tracers

108 The focusing of this paper will be the comparison and validation of the performances of MO and
109 SCSOFS in the SCS, based on the observation data we have got in 2012. The rest of this paper is
110 organized as follows. Section 2 gives the introductions to the observed data which are employed to
111 validate the systems, and the configurations of MO and SCSOFS. Section 3 shows the results of
112 comparison and validation and discussions. Section 4 presents the summary and conclusions.

113 2 Observed data and numerical operational systems

114 2.1 Satellite data

115 The Map of Sea Level Anomaly (MSLA) and Map of Absolute Dynamic Topography (MADT) data, also
116 with the relative Geostrophic Velocity Anomaly (GVA) and Absolute Geostrophic Velocity (AGV) data
117 derived from them, respectively, are used to analysis the mesoscale eddy in the SCS and compare with
118 the numerical simulations. They are all-sat-merged and gridded delayed-time altimeter product produced
119 by SSALTO/DUACS and distributed by Aviso in April 2014, with support from Centre National
120 D'études Spatiales (Cnes, www.aviso.altimetry.fr). The products are ~~directly computed~~ on a $0.25^{\circ} \times 0.25^{\circ}$
121 ~~spatial~~ resolution Cartesian grid in both longitude and latitude, ~~with a daily~~ temporal resolution. Its
122 period covers from 1993 to present, and the period of reference has been changed from 7 years
123 (1993-1999) to 20 years (1993-2012). It has been corrected for instrumental errors, environmental
124 perturbations, the ocean sea state influence, the tide influence, atmospheric pressure and multi-mission
125 cross-calibration (CLS, 2015).

126 Two kinds of Sea Surface Temperature (SST) data will be used in this paper. One is derived from the
127 merged satellite's ~~infrared sensors (AVHRR/NOAA) and microwave sensor (AMSR-E/AQUA)~~, and
128 ~~in-situ SST (buoy and ship)~~ data Global Daily SST (MGDSST), with a $0.25^{\circ} \times 0.25^{\circ}$ horizontal resolution,
129 which is analyzed and published ~~at the Office of Marine Prediction of the~~ Japan Meteorological Agency
130 (JMA). The data can be obtained from <http://near-goos1.jodc.go.jp/>.

131 The other one is derived from the NOAA ~~$0.25^{\circ} \times 0.25^{\circ}$~~ daily Optimum Interpolation Sea Surface
132 Temperature (OISST), which is an analysis constructed by combining observations from different
133 platforms, such as satellites, ships, buoys, on a regular grid via optimum interpolation. Right now,
134 National Centers for Environmental Information (NCEI) provides two kinds of OISST: one uses infrared
135 satellite data from the Advanced Very High Resolution Radiometer (AVHRR) named as AVHRR-only,

删除的内容: sampled

删除的内容: from the Mercator gridded product

删除的内容: /AVHRR,

删除的内容: MetOp/AVHRR, GCOMW1/AMSR2,
Coriolis/WINDSAT

删除的内容: by

删除的内容: 1/4

143 and the other one uses AVHRR data along with microwave data from the Advanced Microwave
144 Scanning Radiometer (AMSR) on the Earth Observing System Aqua or AMSR-E satellite named as
145 AVHRR+AMSR. ~~Since the production of the AVHRR+AMSR data ended in 2011, the first one,~~
146 AVHRR-only, is used in this study, which spans 1981 to the present and can be downloaded from the
147 website <http://www.ncdc.noaa.gov/oisst/data-access>.

删除的内容: T

148 2.2 In-situ data

149 The *in-situ* data employed in this paper for the comparison and validation of both systems are provided
150 by the South China Sea Institute of Oceanology, Chinese Academy of Sciences. There were one mooring
151 to measure the sea water velocity and 5 cruises implemented to measure the temperature and salinity (TS)
152 in the SCS during 2012.

153 The mooring station is located at Maoming (Fig. 1), where bottom-mounted upward-looking 75 kHz
154 Acoustic Doppler Current Profilers (ADCPs) are deployed to monitor the current profile (U component
155 and V component) from the depth of 2_m to 48_m with a 2-m interval in vertical. The period of the
156 monitoring is from 11 July to 8 October, in 2012, with a temporal interval 10 min. Firstly, the ~~outlier~~ data
157 are eliminated from the original measured data; in the second, a low-pass filter with 25-hour is applied to
158 filter out the tidal current; and a 25-hour average is calculated to get the daily average data, in order to
159 compare and validate with the simulated results of MO and SCSOFS.

删除的内容: abnormal

160 The TS data from 5 cruises are measured by SeaBird 19 plus conductivity-temperature-depth (CTD) with
161 1-m resolution in vertical. Among the 5 cruises, one is the Qiongdong cruise in the NSCS, which was
162 conducted 9 days from 12 to 20 July at 90 stations along 6 sections (~~see Fig.1~~); another one is the Nansha
163 cruise around the Nansha Islands, which was conducted 5 days from 24 to 28 August at 17 stations along
164 10°N section from 109.5°E to 117.5°E. The TS data from those two cruises will be used to compare and

删除的内容: S

165 validate the TS distribution from MO and SCSOFS in vertical and horizontal. ~~The TS data collected~~
166 from ~~all the 5~~ cruises will be ~~used to perform a correlation analysis of each of the simulated predictions of~~
167 ~~MO and SCSOFS models with the observations.~~

删除的内容: All the measured

删除的内容: collected

删除的内容: compare with the simulated data from

删除的内容: via correlation analysis

168 2.3 The configurations of SCSOFS

169 The SCSOFS is build up based on the Regional Ocean Modeling System (ROMS), which is a
170 three-dimensional, non-linear primitive equations, free surface, hydrostatic, split-explicit,

删除的内容: ic

删除的内容: l

180 topography-following-coordinate in vertical and orthogonal curvilinear in horizontal on a staggered
181 Arakawa C-grid (Arakawa and Lamb, 1977) oceanic model (Shchepetkin and McWilliams, 2005).
182 To avoid the influences of boundary to the circulations in the SCS, the model's boundaries was extended
183 to southward and eastward, then the model covered a larger domain (4.5°S to 28.3°N, 99°E to 145°E, Fig.
184 1) than the SCS. The horizontal resolution variates from 1/12° in the south and east boundary to 1/30° in
185 the SCS. There were 36 s-coordinate levels in the vertical with the thinnest layer being 0.16 m on the
186 surface. The bathymetry was extracted from the ETOPO1 data sets published by U.S. National
187 Geophysical Data Center (NGDC), which is a global relief model of Earth's surface that integrates ocean
188 bathymetry and land topography, with 1 arc-minute resolution (Amante and Eakins, 2009). The ETOPO1
189 data has combined the satellite altimeter observations, shipping load sonar measurement, multi
190 resolutions digital terrain database and the global digital terrain model and many other sources, and been
191 used in the global and regional oceanic model widely. And the original bathymetry was revised in the
192 area of next to the coast of China mainland according to the *in-situ* data measured by our group, then
193 smoothed according to Shapiro (1975). The maximum depth was set to be 6000 m and the minimum
194 depth to be 10 m in the model (Wang, 1996).

195 The initial temperature and salinity were derived from the climatology monthly mean SODA in January.
196 However, the initial velocities and elevation were set to zero, which means to integrate the model from a
197 static status. The model's western lateral boundary was treated as a wall. The other three (northern,
198 southern, eastern) lateral boundaries were opened, whose temperature, salinity, velocity, and elevation
199 were prescribed by spatial interpolation of the monthly mean SODA dataset. The 2D and 3D velocities,
200 through the open boundaries, are modulated to guarantee the conservation of volume flux in the whole
201 model domain. In addition, the nudging technology was used for 3D velocity, temperature, and salinity to
202 the three open lateral boundaries with a 30-day time scale for outflow and 3-day for inflow.
203 The model is forced using 6-hourly wind stress, net fresh water flux, net heat flux, surface solar
204 shortwave radiation at surface from NCEP_Reanalysis 2 data provided by the NOAA/OAR/ESRL PSD,
205 Boulder, Colorado, USA, from their web site at <http://www.esrl.noaa.gov/psd/> (Kanamitsu et al., 2002).
206 In order to get more reasonable simulated SST, the kinematic surface net heat flux sensitivity to SST
207 ($dQ/dSST$) is used to introduce thermal feedback to correct net surface heat flux (Barnier et al., 1995)
208 with a constant number $-30 \text{ W/m}^2/\text{C}$ in the whole domain. The MGDSST data is used to correct net

删除的内容: Simple Ocean Data Assimilation (

删除的内容: . Carton and Giese, 2008)

211 [surface heat flux](#). In addition, the monthly mean climatology discharges of the Mekong River and the
212 Pearl River are prescribed to the model.

213 The system was run with 6 seconds time step for the external mode, and 180 seconds for the internal
214 mode under the initial conditions, boundary conditions and surface forcing mentioned in above. The
215 system was conducted a hindcast run from 2000 to 2011 after a 15 years climatology run for spin-up
216 (Wang et al., 2012). The model results are archived to the snapshot with a 5-day interval, which will be
217 used as the ensemble members for the EnOI (Ensemble Optimal Interpolation) method assimilation.
218 After the hindcast run, the system was conducted an assimilation run in 2012 with EnOI method, the
219 along track SLA data from AVISO had been assimilated as the observations with a 7-day time window.
220 The details on the EnOI applied in the SCSOFS can be referred as Ji et al. (2015). The assimilated results
221 are archived to daily mean with a 1-day interval in 2012, which will be used to compare and validate in
222 this paper. Then the system is operating in NMEFC since January 1st, 2013. It runs daily for 6 days
223 (1-day nowcast and 5-day forecast), and provides 120-hour forecasting products, which including the 3D
224 ocean temperature, salinity and currents with 24 hours interval.

225 **2.4 The configurations of MO**

226 The high resolution global analysis and forecasting system PSY4V1R3 was operational as the V2 of the
227 MyOcean project from February 2011 up to April 2013, when it was replaced by the PSY4V2R2 system.
228 During this period, PSY4V1R3 has been producing weekly 14-day hindcasts and daily 7-day forecasts.

229 [The PSY4V1R3 configuration described as followed is indicated for as MO model through this paper.](#)

230 The model configuration of PSY4V1R3 is based on a tripolar ORCA grid type (Madec and Imbard, 1996)
231 in the NEMO 1.09 version with a $1/12^\circ$ horizontal resolution which means 9 km at the Equator, 7 km at
232 mid latitudes and 2km toward the Ross and Weddel Sea. The grid cells follow an Arakawa C-grid type,

233 The 50-level vertical discretization retained in this system has 1m resolution at the surface, decreasing to
234 450_m at the bottom and 22 levels within the upper 100_m. "Partial cell" parametrization was chosen for
235 a better representation of the topographic floor (Barnier et al., 2006). The high frequency gravity waves
236 are filtered out by the free surface formulation of Roulet and Madec (2000).

237 For the diffusion, a horizontal bilaplacian was added along the equator ($20\text{ m}^2\text{s}^{-1}$) and two laplacians in
238 the Canadian straits (up to $100\text{ m}^2\text{s}^{-1}$). Laplacian lateral isopycnal diffusion was added on tracers (125
239 m^2s^{-1}) and a horizontal biharmonic viscosity was added for the momentum ($-1\times 10^{10}\text{ m}^4\text{s}^{-1}$ at the

删除的内容: (Arakawa and Lamb, 1977)

241 Equator and decreasing poleward as the cube of the grid size). In addition, the vertical mixing is
242 parameterized according to a turbulent closure model (TKE order 1.5) adapted by Blanke and Delecluse
243 (1993), the lateral friction condition is a partial-slip condition with a regionalization for the
244 Mediterranean Sea, Indonesian region, Canadian straits and Cape Horn. The atmospheric fields are taken
245 from the ECMWF (European Centre for Medium Range Weather Forecasts) Integrated Forecast System
246 at a daily average frequency. Momentum and heat turbulent surface fluxes are computed from CLIO bulk
247 formulae (Goosse et al., 2001). We use a viscous-plastic rheology formulation for the LIM2_VP ice
248 model (Fichefet and Maqueda, 1997, LIM2_VP in Hunke and Dukowicz 1997). A multivariate data
249 assimilation (Kalman Filter kernel with SEEK formulation, Pham et al., 1998) of *in-situ* T and S (from
250 Coriolis/Ifremer), along-track MSLA (from AVISO, with MDT from Rio and Hernandez, 2004) and
251 intermediate resolution SST ($0.25^\circ \times 0.25^\circ$ SST product RTG from NOAA) is performed with the SAM2
252 software (Lellouche et al., 2013). An Incremental Analysis Update (IAU) centered on the 4th day of the
253 7-day assimilation window ensures a smooth correction of T, S, U, V and SSH (Sea Surface Height). The
254 assimilation cycle consists of a first 7-day simulation called guess or forecast, at the end of which the
255 analysis takes place. The IAU correction is then computed and the model is re-run on the same week,
256 progressively adding the correction. The increment is distributed in time with a Gaussian shape which is
257 centered on the 4th day. More details on the SAM2 software (applied on other model configurations) can
258 be found in Lellouche et al. (2013) except that no large scale bias correction is applied in PSY4V1R3.
259 Concerning the initial conditions, the PSY4V1R3 was started in April 2009 from a 3D climatology of
260 temperature and salinity (WOA2005, Antonov et al., 2006; Locarnini et al., 2006).

261 3 Comparisons, validations and discussion

262 3.1 Velocities

263 3.1.1 Absolute Geostrophic Velocity

264 Figure 2 shows the distributions of the monthly AGV composited with SSH from AVISO, MO, and
265 SCSOFS in January, April, July, and October of 2012, respectively. Here we use the January, April, July,
266 and October represent winter, spring, summer, and autumn, respectively. It is valuable to note that the
267 AGV of MO and SCSOFS are not the velocities output from the numerical model directive. However, in

删除的内容: .

删除的内容:

删除的内容: 1/4

带格式的: 字体: 非加粗

删除的内容: Sea Surface Height (

删除的内容:)

273 order to better comparison, they are recalculated according to SSH from the model output on every day
274 and assuming geostrophic balance following Eq. (1):

$$275 \quad u = -\frac{g}{f} \frac{\partial SSH}{\partial y} \quad v = \frac{g}{f} \frac{\partial SSH}{\partial x} \quad (1)$$

276 where g is gravitation acceleration, f is the Coriolis parameter, x, y are the east, north axis; u, v are the
277 eastward, northward velocity components in horizontal, respectively.

278 By comparing among the three results, both MO and SCSOFS can catch the main basin-scale oceanic
279 circulation pattern in the SCS, and show that a cyclonic gyre in winter and an anti-cyclonic gyre in
280 summer, which being well accordance with the pattern of AVISO. It is worth to mention that the result of
281 MO is well agreement with the AVSIO in January, such as the southward western boundary currents
282 along the eastern coast of Vietnam, the LCC, the anti-cyclonic eddy in the western of the LUS around
283 (118°E, 21°N), the cyclonic eddy in the eastern of the Vietnam around (113°E, 15°N). However, the
284 result of SCSOFS is much smooth without obvious mesoscale or small scale circulation, or they are very
285 weaker (0.2-0.4 m s⁻¹) than those (0.6-0.8 m s⁻¹) of AVISO or MO. The circulation is chaos in spring in
286 the SCS, though the circulation pattern of MO is better agreement with the one of AVISO than the one of
287 SCSOFS. All the three results show the anti-cyclonic eddy around (111°E, 10°N) and the western
288 boundary jet in the southeast of the Vietnam in summer, with the maximum speed being about 1.0 m s⁻¹,
289 0.9 m s⁻¹, and 0.7 m s⁻¹ for AVISO, MO, SCSOFS, respectively. The westward intensification along the
290 eastern coast of the Vietnam is most obvious in autumn than other three seasons, and the maximum speed
291 is more than 1.0 m s⁻¹ for MO and SCSOFS, but 0.7 m s⁻¹ for AVISO.

292 As mentioned in Sect. 1, the Kuroshio intruding the SCS through the LUS has been distinguished three
293 types as the looping path, the leaking path and the leaping path, according to Nan et al. (2011a). All three
294 results show the looping path in winter, the leaping path in summer and leaking path in autumn, which is
295 well accordance with the model results showed by Wu and Chiang (2007). However, AVISO, MO, and
296 SCSOFS show the leaking path, looping path, and leaping path in spring, respectively.

297 3.1.2 Time series from mooring station

298 Figure 3 shows the comparison of the daily mean time series of the u, v components from the mooring,
299 MO, and SCSOFS in 40m-depth layer at the Maoming station (see Fig. 1) from July 11 to October 8,
300 2012. Both MO and SCSOFS can catch the same variation trends of the time series with the mooring
301 observation. Especially, MO results have represented the current variations well for both u - and v -

删除的内容: , except that the current speeds are a little stronger than AVISO

删除的内容: S

305 component, during the period of the Typhoon Kai-tak on 17 August 2012. Although SCSOFS shows the
306 larger velocity during the Typhoon Kai-tak, the magnitude of speed is less than the observation and
307 anticipating the observation about 1 day. The root mean square errors (RMSE) between MO and
308 SCSOFS and observation are 0.075_m s⁻¹, 0.094_m s⁻¹ for u-component, 0.062_m s⁻¹, 0.084m s⁻¹ for
309 v-component, respectively. Overall, MO results are better agreement with the observation than those of
310 SCSOFS. However, SCSOFS results have a temporal bias comparing with the observation, which is
311 leading the observation about 1 day.

删除的内容: range of large

带格式的: 字体: 非加粗

删除的内容: leading

删除的内容: phase

312 3.2 Temperature and Salinity

313 3.2.1 SST

314 SST is a very important prognostic variable in a hydrostatic ocean general circulation numerical model,
315 which plays a key role to the ocean circulations and the air-sea interaction. So SST error is crucial criteria
316 of the numerical model skill, especially for an operational ocean circulation model. In fact, the SST
317 simulation error is affected by several factors, for example the limitation of physical model, the surface
318 atmosphere forcing, the bias of initial field and the uncertainty from the open boundary, as pointed out by
319 Ji et al. (2015). Although the SST data have been assimilated into both MO and SCSOFS, the assimilated
320 SST still has some errors for both systems.

321 Figure 4 shows the distributions of the monthly mean SST errors between two systems and MGDSST in
322 the SCS in 2012. The errors show an obvious regional distribution, the bigger errors mainly exist in the
323 coastal region for the depth shallower than 200 m, such as in the TWS, the eastern of the Guangdong
324 province in January, the gulf of Tonkin in July. What's more, the strong seasonal variation for the
325 basin-averaged SST error also can be found, which is larger in winter and smaller in summer, from both
326 systems. Comparing with MGDSST, the maximum, minimum, and mean for the basin-averaged 12
327 monthly RMSEs are 0.78_°C, 0.37_°C, 0.51_°C for the MO, 1.15_°C, 0.56_°C, 0.86_°C for the SCSOFS,
328 respectively, in the SCS. Based on the Fig. 4, the simulated SST performance of MO is better than those
329 of SCSOFS by comparing with MGDSST.

330 3.2.2 Horizontal and vertical distribution of TS

331 The horizontal distributions of 10-m depth layer TS in the eastern of Hainan island from the *in-situ* of
332 Qiongdong cruise, MO, and SCSOFS, respectively, are shown in Fig. 5. Two clear cold and salty water

336 cores located at the eastern of Hainan island, which being about (110.75°E, 19.2°N) and (111.3°E,
337 19.7°N), are shown in both *in-situ* and SCSOFS (Fig. 5), except that the SCSOFS being more saline than
338 *in-situ*. It can be easily deduced that the two cores are produced by upwelling process from the TS
339 vertical distributions of the section K, F, H, and G (Jing et al., 2015).

340 Figure 6 shows the vertical TS distributions from the *in-situ* of Qiongdong cruise, MO and SCSOFS,
341 along section E. Both systems have got the same vertical structures of TS with the *in-situ*. All of them
342 show out the obvious upwelling system, with cold and salty waters flowing from offshore to nearshore
343 along the bottom. All three results show the upper mixing layer depth is about 15_m, with the sea water
344 well mixed above 15_m depth and the isotherms and isohalines are almost vertical, indicating strong
345 stratification in summer. The diluted water is flushing from the nearshore to offshore, with the
346 33-isohaline ~~cross with the sea surface at the position of about 50 km from the coast~~ for both *in-situ* and
347 SCSOFS, but at ~~the position of about 40 km~~ for MO. In above, it is indicated that the results of SCSOFS
348 is better agreement with the *in-situ* than those of MO.

349 The vertical distributions of TS from the *in-situ* of Nansha cruise, MO, and SCSOFS along the 10°N
350 section are shown in Fig.7 for the layer above 300_m and Fig.8 for the layer of 300-1200_m. Both systems
351 have got almost the same vertical structures with the *in-situ*, especially for the upper mixing layer depth
352 about 70_m are shown in the three results. The temperature almost linearly decreases from 28_°C to 3_°C
353 with the depth increasing from the bottom of the upper mixing layer to the 1200_m depth. However, the
354 salinity increases from 33.5 to 34.5 with the depth increasing from the bottom of the upper mixing layer
355 to about 200m depth, and keeps 34.5 from 200_m to 300_m depth. Then a fresh water layer exists in the
356 middle layer from about 400_m to 700_m with the salinity about 34.4. Below the middle layer, the salinity
357 again increases from 34.4 to 34.58 with the depth increasing from 700_m to 1200_m. It indicates that the
358 results of MO and SCSOFS are well agreement with *in-situ*, except that the salinity of the fresh water in
359 the middle layer from MO is less than 34.4 and fresher than those of *in-situ* and SCSOFS, but the
360 thickness of the layer is thicker than those of *in-situ* and SCSOFS.

361 3.2.3 Correlation ~~analysis, between model and in-situ~~

362 In order to better compare and validate the performances of the two systems, we collected all the
363 measured TS data from five cruises in the SCS in 2012 to conduct a comprehensive correlation analysis.
364 Figure 9 shows the comparison, of TS between MO, SCSOFS and *in-situ* by scatter points, respectively.

删除的内容: located

删除的内容: 2

删除的内容: ship

删除的内容: of relativity

369 Any point in the Fig.9 is corresponded with two values of temperature or salinity, one is from the *in-situ*
370 along X axis, and the other one is from MO or SCSOFS along Y axis. The correlation coefficients of
371 temperature are 0.987, 0.982, and of salinity are 0.717, 0.897, between MO, SCSOFS and *in-situ*, over
372 the 95% significance level, respectively, which showing the good relativity between MO, SCSOFS and
373 *in-situ*. It also indicates that the relativity of temperature is better agreement with *in-situ* than those of
374 salinity for both MO and SCSOFS, and SCSOFS is better agreement with *in-situ* than MO for salinity.

375 3.3 Mesoscale activities

376 3.3.1 SST front

377 Oceanic front is a good indicator for connection between water masses with different hydrological
378 features, which is an important marine mesoscale phenomenon. There are numerous SST fronts in the
379 SCS, most of them located on the continental shelf with the depth below 200_m or aligned with the shelf
380 break, especially in the NSCS. A few evident SST fronts have been identified from the long-term
381 NOAA/NASA Pathfinder SST data, namely: Fujian-Guangdong Coastal Front, Pear River Estuary
382 Coastal Front, Taiwan Bank Front, Kuroshio Intrusion Front, Hainan Island East Coastal Front, Tonkin
383 Gulf Coastal Front (Wang et al., 2001). All of them exhibit very strong seasonal variability, which is
384 mainly due to the EAM (Belkin and Cornillon, 2003).

385 Figure 10 shows the distributions of SST fronts from MO and SCSOFS for four seasons. The similar
386 frontal patterns with their evident seasonal variations are shown in both systems, except for some small
387 differences. In winter, most fronts reach maximum strength ($>0.2\text{ }^{\circ}\text{C}/\text{km}$). The Fujian-Guangdong
388 Coastal Front and Taiwan Bank Front are major fronts in the SCS which agree with previous satellite
389 result from Wang et al. (2001). These two fronts merge and extend to Pearl River Estuary and the Hainan
390 Island. The Hainan Island East Coastal Front is stronger in MO than in SCSOFS, whereas the Tonkin
391 Gulf Coastal Front is stronger in SCSOFS than in MO. In SCSOFS, the Kuroshio Intrusion front is
392 obvious, however, which is hardly seen in MO. In spring, most fronts become weak obviously due to the
393 weakening of northeast monsoon from both systems, except that the Hainan West Coastal Front
394 emerges in SCSOFS. In summer, weakening almost occurs in all the fronts mentioned above for
395 SCSOFS, which is in agreement with the result of Wang et al. (2001). However, disappearing occurs in
396 all the fronts for MO. In fall, most fronts fade and disappear, except that the Taiwan Bank front has very

删除的内容: c

删除的内容: f

删除的内容: f

删除的内容: f

401 weak strength compared to other seasons for both systems. Both systems have not shown the Kuroshio
402 Intrusion Front identified by Wang et al. (2001) in summer and fall.

403 3.3.2 The Typhoon Tembin

404 There are a lot of typhoons in the SCS during the typhoon season in every year, so that the typhoon
405 activities are very frequent in the SCS, especially in 2012. One important study on the air-sea interaction
406 is the responding of the physical ocean dynamics to typhoon in the oceanic upper layer. One important
407 responding is the decreasing of SST due to the strong vertical mixing caused by typhoon (Price et al.,
408 1994). According to the SST observation from the satellite, SST usually decreases 2-5_°C due to typhoon
409 passing (Cione and Uhlhorn, 2003; D'Asaro et al., 2007; Wu et al., 2008; Jiang et al., 2009). Dare and
410 McBride (2011) researched the response of SST to the global typhoons during 1981~2008 and indicated
411 that the maximum decreasing of SST usually occurred in 1-day after typhoon passing.

412 In this section, we select the typhoon Tembin as an example to validate the MO and SCSOFS model skill
413 for the SST simulation. As shown in Fig. 11, the typhoon Tembin went through and made a perfect turn
414 around in the NSCS from 25 to 28 August 2012. From the three results, we can find the obvious
415 decreasing of SST 1-day after typhoon passing, which is about 2-4_°C and well correspondence with
416 previous studies mentioned in above. SCSOFS is much better agreement with OISST than MO,
417 especially on 26 and 27 August 2012, not only for the range of SST decreasing, but also for the domain of
418 SST decrease.

419 3.3.3 Mesoscale eddy

420 Mesoscale eddies cannot be identified and extracted from geophysical turbulent flow as observed by
421 satellite altimetry without suitable definition and a competitive identification algorithm. A multitude of
422 different techniques for automatic identification of eddies have been proposed based either on physical or
423 geometric criteria of the flow field. In this study, a free-threshold eddy identification algorithm with the
424 SLA data is employed. This algorithm is based on the vector geometry method and Okubo-Weiss method
425 (Okubo, 1970; Weiss, 1991) with six constraints applied to the SLA to detect an eddy: (1) a
426 vorticity-dominated region at the eddy center ($W < 0$, here W is the Okubo-Weiss parameter, for its
427 definition referred as Xiu et al.(2010)) must exist; (2) the SLA magnitude has a local extreme value
428 (minimum or maximum); (3) closed contours of SLA around the eddy center must exist; (4) the eddy

删除的内容: hot

删除的内容: ing

431 radius must be larger than 45km.(5)the eddy amplitude must be larger than 4cm. In this study, the
432 amplitude is defined as the absolute value of the SLA difference between the eddy center and the SLA
433 along the eddy edge. The Eddy-tracking method used is the one developed by Chaigneau et al. (2008),
434 and we only keep eddies with life span not less than 28 days. Eddies were analyzed and compared based
435 on MO, AVISO and SCSOFS in 2012. The numbers of eddies for three types of data were in Table 1,
436 cyclones and anti-cyclones were counted separately and seasonally.

437 The spatial distribution of eddy birthplace is shown in Fig 12. MO has more eddies formed, especially
438 anti-cyclones formed than those of AVISO, most of the excessive eddy cores were found near the middle
439 of SCS. SCSOFS has more anti-cyclones as well and less cyclones than AVISO. Both MO and SCSOFS
440 show excessive eddies formed in the middle of the basin and less eddies in the western of the east of
441 Vietnam. The SLA of SCSOFS and MO is calculated simply by subtracting mean SSH (4 years mean
442 for SCSOFS and only one-year mean for MO) instead of an uniformed Mean Sea Surface, which might
443 cause the excessive anti-cyclones in both models. All three types of data agree that less eddies formed in
444 the middle part of NSCS.

445 As for the seasonal distributions (figures not shown), all three data have most eddies in spring. Both
446 AVISO and SCSOFS have ~~lest eddies in fall, and~~ more cyclones than anti-cyclones in spring and fall, and
447 all three have less cyclones ~~than anti-cyclones~~ in summer. SCSOFS differs with AVISO mainly in winter
448 while they agree reasonably in the other three seasons. MO has surplus eddies counted in every season
449 especially for anti-cyclones, which might because of the error introduced by the simplified calculation of
450 SLA.

451 4 Conclusions

452 Two operational ocean analysis and forecasting systems, MO and SCSOFS, have been built based on the
453 state-of-the-art hydrodynamic ocean model in France and China, respectively. The comparison and
454 validation for the performance of both systems on the ocean circulation, the structures of the TS, and
455 mesoscale activities in the SCS, based on the observed satellite and *in-situ* data in 2012, are shown in this
456 paper. The comprehensive performances for the both systems are summarized as follow.

457 Both systems have caught the main basin-scale circulations in the SCS and been well agreement with the
458 result of AVISO. And the results of MO are better agreement with those of AVISO than those of

删除的内容: 2

删除的内容: and lest in fall

461 SCSOFS for several branches and eddies in January. There are no many mesoscale or small scale
462 circulations shown in SCSOFS, which may because of a little strong horizontal mixing set in the model.
463 The westward intensification in the eastern coast of the Vietnam is most strong in autumn among the four
464 seasons. For the type of the Kuroshio intruding the SCS, the three results show the looping path in winter,
465 the leaping path in summer and leaking path in autumn. However, the leaking path, looping path and
466 leaping path are shown for AVISO, MO and SCSOFS in spring, respectively.

467 Both systems get the same variation of the u-/v- components time series with the mooring observation.
468 The RMSE between MO, SCSOFS and mooring observation are 0.075_m/s, 0.094_m/s for u-component,
469 0.062_m/s, 0.084_m/s for v-component, respectively. The results of MO are better agreement with the
470 observation than those of SCSOFS, especially during the period of the Typhoon Kai-tak.

471 The maximum, minimum, and mean for the basin-averaged 12 monthly RMSEs between MO and
472 MGDSST are 0.78_°C, 0.37_°C, 0.51_°C, between SCSOFS and MGDSST are 1.15_°C, 0.56_°C, 0.86_°C, in
473 the SCS, respectively. For the horizontal and vertical distributions of TS, both systems have got the same
474 structures with the *in-situ*, but the results of SCSOFS are better agreement with the *in-situ* than those of
475 MO. The correlation coefficients of temperature are 0.987, 0.982, and of salinity are 0.717, 0.897,
476 between MO, SCSOFS and *in-situ*, over the 95% significance level, respectively. It indicates that the
477 good relativity between MO, SCSOFS and *in-situ*, the relativity of temperature is better agreement with
478 *in-situ* than those of salinity for both MO and SCSOFS, and SCSOFS is better agreement with *in-situ*
479 than MO for salinity.

480 The similar SST frontal patterns with their evident seasonal variations are shown in both systems. Most
481 fronts achieve maximum strength in winter, become weak obviously due to the weakening of northeaster
482 monsoon EAM in spring and summer, fade and disappear in autumn. It is well agreement with the result
483 of Wang et al. (2001).

484 During the typhoon Tembin in the NSCS, the obvious decreasing of SST about 2-4_°C occurs 1-day after
485 typhoon passing shown in the results of MO, SCSOFS and OISST, which is well agreement with
486 previous studies. SCSOFS is much better agreement with OISST than MO both for the range and domain
487 of SST decreasing.

488 MO has more eddies formed near the middle of SCS than AVISO, especially for anti-cyclones. SCSOFS
489 has more anti-cyclones as well, but less cyclones than AVISO. All three data have most eddies in spring

删除的内容: for the SCSOFS

491 and lest in fall, and less cyclones than anti-cyclones in summer. Both AVISO and SCSOFS have more
492 cyclones than anti-cyclones in spring and fall.

493 In order to improve their performances further in the SCS, according to the comparison and validation for
494 the two systems, MO and SCSOFS, we would like to propose some suggestions to modify the systems.

495 For MO, we would like to suggest (1) to modify the model bathymetry in the coast area for the depth less
496 than 200m to improve the model performance in shallow water area, such as SST front; (2) to change the
497 initial conditions of TS to improve the TS vertical structures, especially for the salinity in deep water area;

498 For SCSOFS, we would like to suggest (1) to weaken horizontal mixing to get more reasonable
499 mesoscale or small scale circulations; (2) to optimize the data assimilation scheme further to better
500 assimilate the *in-situ* and satellite data; (3) to replace the surface forcing data with the higher horizontal
501 or temporal resolution; (4) to replace the boundary conditions from monthly to weekly or daily, such as
502 MO. For both systems, we also would like to suggest to try to get and assimilate more observed data
503 during the typhoon period to catch the typhoon process more exactly.

504 **Author contribution**

505 X. Zhu, H. Wang and G. Liu compared and validated the model results on velocities and TS. C.
506 Régnier and M. Drévillon build the MO, D. Wang build the SCSOFS. X. Kuang analyzed the model
507 results on mesoscale eddy. S. Ren analyzed the model results on SST front. Z. Jing provided the *in-situ*
508 data. X. Zhu prepared the manuscript with contributions from all co-authors.

509 **Acknowledgements**

510 We would like to thank the anonymous reviewers and the Editor, , for their valuable contributions
511 that allow us to improve the manuscript substantially. This study is supported by the National Natural
512 Science Foundation of China under contract No. 41222038, 41376016, 41206023 and the
513 Strategic Priority Research Program of the Chinese Academy of Sciences Grant No. XDA1102010403.

514 **References**

515 Arakawa, A. and Lamb, V. R.: Computational design of the basic dynamical processes of the UCLA
516 general circulation model. *Methods of Computational Physics*, 17. New York: Academic Press, 173–
517 265, 1977.

518 Amante, C. and Eakins, B.: ETOPO1 1 Arc-Minute Global Relief Model: Procedures, Data Sources and
519 Analysis. NOAA Technical Memorandum NESDIS NGDC-24. National Geophysical Data Center,
520 NOAA, doi:10.7289/V5C8276M, 2009.

521 [Antonov, J. I., Locarnini, R. A., Boyer, T. P., Mishonov, A. V., and Garcia, H. E.: World Ocean Atlas](#)
522 [2005, Volume 2: Salinity. S. Levitus, Ed. NOAA Atlas NESDIS 62, U.S. Government Printing Office,](#)
523 [Washington, D.C., 182 pp. 2006.](#)

524 [Barnier, B., Siefridt, L., Marchesiello, P.: Thermal forcing for a global ocean circulation model using a](#)
525 [three-year climatology of ECMWF analyses. *J. Mar. Syst.* 6 \(4\), 363–380.](#)
526 [http://dx.doi.org/10.1016/0924-7963\(94\)00034-9](http://dx.doi.org/10.1016/0924-7963(94)00034-9), 1995.

527 Barnier, B., Madec, G., Penduff, T., Molines, J. M., Treguier, A. M., Le Sommer, J., Beckmann, A.,
528 Biastoch, A., Boning, C., Deng, J., Derval, C., Durand, E., Gulev, S., Remy, E., Talandier, C., Theetten,
529 S., Maltrud, M., McClean, J., and De Cuevas, B.: Impact of partial steps and momentum advection
530 schemes in a global circulation model at eddy permitting resolution, *Ocean Dynam.*, 56, 543–567, 2006.

531 Belkin, I. and Cornillon, P.: SST fronts of the Pacific coastal and marginal seas. *Pacific Oceanogr.*,
532 1(2):90–113, 2003.

533 ~~Blanke, B. and Delecluse, P.: Variability of the tropical Atlantic-Ocean simulated by a general-~~
534 ~~circulation model with 2 different mixed-layer physics, *J. Phys. Oceanogr.*, 23, 1363–1388, 1993.~~

535 Cai, S. and Wang, W.: A numerical study on the circulation mechanism in the northeastern South China
536 Sea and Taiwan Strait. *Tropic Oceanology*, 16(1), 7–15, 1997. (in Chinese with English abstract).

537 Carton, J. and Giese, B.: A Reanalysis of Ocean Climate Using Simple Ocean Data Assimilation
538 (SODA). *Mon. Weath. Rev.*, 136, 2999–3017, doi: 10.1175/2007MWR1978.1, 2008.

539 Caruso, M., Gawarkiewicz, G. and Beardsley, R.: Interannual variability of the Kuroshio intrusion in the
540 South China Sea. *J. Oceanogr.*, 62(4), 559–575, 2006.

541 Chaigneau, A., Gizolme, A. and Grados, C.: Mesoscale eddies off Peru in altimeter records:
542 Identification algorithms and eddy spatiotemporal patterns, *Prog. Oceanogr.*, 79, 106–119, 2008.

删除的内容: Bell, M. J., Schiller, A., Traon, P. Y. Le, Smith, N. R.,
Dombrowsky, E. and WilmerBecker, K.: An introduction to GODAE
OceanView. *Journal of Operational Oceanography*, 8, sup1, s2–s11,
doi: 10.1080/1755876X.2015.1022041, 2015. -

547 Chao, S., Shaw, P. and Wang, J.: Wind relaxation as a possible cause of the South China Sea Warm
548 Current. *J. Oceanogr.*, 51(1), 111–132, 1995.

549 Chao, S., Shaw, P. and Wu, S.: Deep water ventilation in the South China Sea. *Deep Sea Res. I*, 43, 445–
550 466, 1996.

551 Chern, C. and Wang, J.: A numerical study of the summertime flow around the Luzon Strait. *J. Oceanogr.*,
552 54(1), 53–64, 1998.

553 Chern, C. and Wang, J.: Numerical study of the upper-layer circulation in the South China Sea. *J*
554 *Oceanogr.*, 59, 11–24, 2003.

555 Chern, C., Jan, S. and Wang, J.: Numerical study of mean flow patterns in the South China Sea and the
556 Luzon Strait, *Ocean Dynamics*, 60, 1 047–1 059, doi:10.1007/s10236-010-0305-3, 2010.

557 Chu, P. and Li, R.: South China Sea Isopycnal-Surface Circulation. *J. Phys. Oceanogr.*, 30, 2420–2438,
558 2000.

559 Chu, P., Lu, S. and Chen, Y.: A Coastal Air-Ocean Coupled System (CAOCS) evaluated using an
560 Airborne Expendable Bathythermograph (AXBT) data set, *J. Oceanogr.*, 55, 543–558,
561 doi:10.1023/A:1007847609139, 1999.

562 Cione, J. and Uhlhorn, E.: Sea surface temperature variability in hurricanes: Implications with respect to
563 intensity change. *Monthly Weather Review*, 131(8), 1783–1796, 2003.

564 CLS, SSALTO/DUACS User handbook: (M)SLA and (M)ADT Near-Real Time and Delayed Time
565 Products. CLS-DOS-NT-06-034, Issue 4.4, Nomenclature: SALP-MU-P-EA-21065-CLS, 2015.

566 Dare, R. and McBride, J.: Sea surface temperature response to tropical cyclones. *Monthly Weather*
567 *Review*, 139(12), 3798–3808, 2011.

568 D’Asaro, E., Sanford, T., Niiler, P., Terrill, E.: Cold wake of hurricane Frances. *Geophys. Res. Lett.*,
569 34(15), L15609, 2007.

570 Du, Y., Yi, J., Wu, D., He, Z., Wang, D., Liang, F.: Mesoscale oceanic eddies in the South China Sea
571 from 1992 to 2012: evolution processes and statistical analysis. *Acta Oceanologica Sinica*, 33(11), 36–
572 47, doi: 10.1007/s13131-014-0530-6, 2014.

573 Fang, G. and Zhao, B.: A note on the main forcing of the northeastward flowing current off the Southeast
574 China Coast. *Prog. Oceanog.*, 21, 363–372, 1988.

575 Fang, Y., Fang, G. and Yu, K.: ADI barotropic ocean model for simulation of Kuroshio intrusion into
576 China southeastern waters. *Chin. J. Oceanol. Limnol.*, 14(4), 357–366, 1996.

删除的内容: Chu, P. and Fan, C.: A low salinity cool-core cyclonic eddy detected northwest of Luzon during the South China Sea Monsoon Experiment (SCSMEX) in July 1998, *J. Oceanogr.*, 57, 549–563, doi:10.1023/A:1021251519067, 2001. .

581 Farris, A. and Wimbush, M.: Wind-induced intrusion into the South China Sea. *J. Oceanogr.*, 52, 771–
582 784, 1996.

583 Fichefet, T. and Maqueda, M. A.: Sensitivity of a global sea ice model to the treatment of ice
584 thermodynamics and dynamics, *J. Geophys. Res.*, 102, 12609–12646, 1997.

585 Goosse, H., Campin, J. M., Deleersnijder, E., Fichefet, T., Mathieu, P. P., Maqueda, M. A. M., and
586 Tartinville, B.: Description of the CLIO model version 3.0, Institut d’Astronomie et de Geophysique
587 Georges Lemaitre, Catholic University of Louvain (Belgium), 2001.

588 Guan, B.: The warm current in the South China Sea—a current flowing against the wind in winter in
589 the open sea off Guangdong province. *Oceanologia et Limnologia Sinica*, 9(2), 117–127, 1978 (in
590 Chinese with English abstract).

591 Guan, B.: Winter counter—wind current off the south eastern China coast and a preliminary
592 investigation of its source. *Proceedings of the Symposium on the Physical and Chemical Oceanography*
593 *of the China Seas*. Beijing, China Ocean Press, 1–9, 1993.

594 Hellerman, S. and Rosenstein, M.: Normal monthly wind stress over the world ocean with error estimates.
595 *J. Phys. Oceanogr.*, 13, 1 093–1 104, 1983.

596 Hu, J., Liang, H. and Zhang, X.: Sectional distribution of salinity and its indication of Kuroshio’s
597 intrusion in southern Taiwan Strait and northern South China Sea late summer, 1994. *Acta Oceanologica*
598 *Sinica*, 18(2), 225–236, 1999.

599 Hu, J., Kawamura, H., Hong, H. and Qi, Y.: A review on the currents in the South China Sea: seasonal
600 circulation, South China Sea Current and Kuroshio intrusion. *J. Oceanogr.*, 56, 607–624, 2000.

601 Hu, J., Gan, J., Sun, Z., Zhu, J. and Dai, M.: Observed three dimensional structure of a cold eddy in the
602 southwestern South China Sea, *J. Geophys. Res.*, 116, C05016, doi:10.1029/2010JC006810, 2011.

603 Huang, Q., Wang, W., Li, Y., Li, C. and Mao, M.: General situations of the current and eddy in the South
604 China Sea. *Advance in Earth Sciences*, 7(5), 1–9, 1992 (in Chinese with English abstract)

605 Hunke, E. C. and Dukowicz J. K.: An elastic-viscous-plastic model for sea ice dynamics, *J. Phys.*
606 *Oceanogr.*, 27, 1849–1867, 1997.

607 Ji, Q., Zhu, X., Wang, H., Liu, G., Gao, S., Ji, X. and Xu, Q.: Assimilating operational SST and sea ice
608 analysis data into an operational circulation model for the coastal seas of China. *Acta oceanologica*
609 *Sinica*, 34(7), 54–64, doi: 10.1007/s13131-015-0691-y, 2015.

610 Jiang, X., Zhong, Z. and Jiang, J.: Upper ocean response of the South China Sea to Typhoon Krovanh
611 (2003). *Dynamics of Atmospheres and Oceans*, 47(1), 165–175, 2009.

612 Jing, Z. Y., Qi, Y. Q., Du, Y., Zhang, S. W. and Xie, L. L.: Summer upwelling and thermal fronts in the
613 northwestern South China Sea: Observational analysis of two mesoscale mapping surveys. *J. Geophys.*
614 *Res. Oceans*, 120, 1993–2006, doi:10.1002/2014JC010601, 2015.

615 Kanamitsu, M., Ebisuzaki, W., Woollen, J., Yang, S., Hnilo, J., Fiorino, M., and Potter, G.: NCEP-DOE
616 AMIP-II Reanalysis (R-2). *Bulletin of the American Meteorological Society*, 1631–1643, Nov 2002.

617 Lellouche, J. M., Le Galloudec, O., Drévilion, M., Régnier, C., Greiner, E., Garric, G., Ferry, N.,
618 Desportes, C., Testut, C. E., Bricaud, C., Bourdalle-Badie, R., Tranchant, B., Benkiran, M., Drillet, Y.,
619 Li, R., Zeng, Q., Gan, Z. and Wang, W.: Numerical simulation of South China Sea Warm Current and
620 currents in Taiwan Strait in winter. *Progress in Natural Sciences*, 3(1), 21–25, 1993. (in Chinese with
621 English abstract).

622 Li, L., Nowlin Jr., W. D. and Su, J.: Anticyclonic rings from the Kuroshio in the South China Sea.
623 *Deep-Sea Res. I*, 45, 1469–1482, 1998a.

624 Li, W., Liu, Q. and Yang, H.: Principal features of ocean circulation in the Luzon Strait. *Journal of Ocean*
625 *University of Qingdao*, 28(3), 345–352, 1998b (in Chinese with English abstract).

626 Liang, W., Yang, Y., Tang, T., and Chuang, W.: Kuroshio in the Luzon Strait. *J. Geophys. Res.*, 113,
627 C08048, doi:10.1029/2007JC004609, 2008.

628 Liu, Q., Liu, C., Zheng, S., Xu, Q. and Li, W.: The deformation of Kuroshio in the Luzon Strait and its
629 dynamics. *Journal of Ocean University of Qingdao*, 26(4), 413–420, 1996. (in Chinese with English
630 abstract).

631 [Locarnini, R. A., Mishonov, A. V., Antonov, J. I., Boyer, T. P., and Garcia, H. E. World Ocean Atlas](#)
632 [2005, Volume 1: Temperature. S. Levitus, Ed. NOAA Atlas NESDIS 61, U.S. Government Printing](#)
633 [Office, Washington, D.C., 182 pp. 2006.](#)

634 Madec, G. and Imbard, M.: A global ocean mesh to overcome the North Pole singularity, *Clim. Dynam.*,
635 12, 381–388, 1996.

636 Mao, Q., Shi, P. and Qi, Y.: Sea surface dynamic topography and geostrophic current over the South
637 China Sea from Geosat altimeter observation. *Acta Oceanologica Sinica*, 21(1), 11–16, 1999. (in Chinese
638 with English abstract).

删除的内容: Daudin, A. and De Nicola, C.: Evaluation of global monitoring and forecasting systems at Mercator Ocean, *Ocean Sci.*, 9, 57–81, doi:10.5194/os-9-57-2013, 2013

642 Nan, F., Xue, H., Chai, F., Shi, L., Shi, M. and Guo, P.: Identification of different types of Kuroshio
643 intrusion into the South China Sea. *Ocean Dynamics*, doi: 10.1007/s10236-011-0426-3, 2011a.

644 Nan, F., He, Z., Zhou, H. and Wang, D.: Three long-lived anticyclonic eddies in the northern South
645 China Sea. *J. Geophys. Res.*, 116, C05002, doi:10.1029/2010JC006790, 2011b.

646 Nan, F., Xue, H., Chai, F., Wang, D., Yu, F., Shi, M., Guo, P. and Xiu, P.: Weakening of the Kuroshio
647 intrusion into the South China Sea over the past two decades. *Journal of Climate*, 26, 8097–8110, doi:
648 10.1175/JCLI-D-12-00315.1, 2013.

649 Nan, F., Xue, H. and Yu, F.: Kuroshio intrusion into the South China Sea: A review. *Progress in*
650 *Oceanography*, 137(A), 314–333, doi: 10.1016/j.pocean.2014.05.012, 2015.

651 Okubo, A.: Horizontal dispersion of floatable particles in the vicinity of velocity singularity such as
652 convergences. *Deep Sea Research*, 17, 445–454, 1970.

653 Pham, D. T., Verron, J., and Roubaud, M. C.: A singular evolutive extended Kalman filter for data
654 assimilation in oceanography, *J. Mar. Syst.*, 16, 323–340, 1998.

655 Price, J., Sanford, T., Forristall, G.: Forced stage response to a moving hurricane. *J. Phys. Oceanogr.*,
656 24(2), 233–260, 1994.

657 Qu, T.: Upper-layer circulation in the South China Sea. *J. Phys. Oceanogr.*, 90, 1450–1460, 2000.

658 Qu, T., Mitsudera, H. and Yamagata, T.: Intrusion of the North Pacific waters into the South China Sea.
659 *J. Geophys. Res.*, 105(C3), 6415–6424, 2000.

660 Rio, M. H., Hernandez F.: A mean dynamic topography computed over the world ocean from altimetry,
661 in situ measurements, and a geoid model, *J. Geophys. Res.*, 109, C12032, 2004

662 Roullet, G. and Madec, G.: Salt conservation, free surface, and varying levels: a new formulation for
663 ocean general circulation models, *J. Geophys. Res.*, 105, 23927–23942, 2000.

664 Shapiro, R.: Linear Filtering. *Math. Comput.*, 29, 1094–1097, 1975.

665 Shchepetkin, A. and McWilliams, J.: The regional oceanic modeling system (ROMS): a split-explicit,
666 free-surface, topography-following-coordinate oceanic model. *Ocean Modell.*, 9, 347–404,
667 doi:10.1016/j.ocemod.2004.08.002, 2005.

668 Su, J.: Overview of the South China Sea circulation and its dynamics. *Acta Oceanologica Sinica*, 27(6),
669 1–8, 2005.

670 Takano, K., Harashima, A. and Namba, T.: A numerical simulation of the circulation in the South China
671 Sea—preliminary results. *Acta Oceanogr. Taiwanica*, 37, 165–186, 1998.

672 Wang, D., Liu, Y., Qi, Y., and Shi, P.: Seasonal variability of thermal fronts in the northern South China
673 Sea from satellite data. *Geophys. Res. Lett.*, 28(20), 3963–3966, 2001.

674 Wang, D., Xu, H., Lin, J. and Hu, J.: Anticyclonic eddies in the northeastern South China Sea during
675 winter 2003/2004. *J. of Oceanogr.*, 64(6), 925–935, 2008.

676 Wang, G., Su, J. and Chu P.: Mesoscale eddies in the South China Sea observed with altimeter data,
677 *Geophys. Res. Lett.*, 30(21), 2121, doi:10.1029/2003GL018532, 2003.

678 Wang, G., Chen, D. and Su, J.: Winter eddy genesis in the Eastern South China Sea due to orographic
679 wind jets. *J. of Phys. Oceanogr.*, 38(3), 726–732, 2008

680 [Wang, H., Wang, Z., Zhu, X., Wang, D., Liu, G., 2012a. Numerical study and prediction of nuclear](#)
681 [contaminant transport from Fukushima Daiichi nuclear power plant in the North Pacific Ocean. *Chin. Sci.*](#)
682 [Bull. 57, 3518–3524. <http://dx.doi.org/10.1007/s11434-012-5171-6>.](#)

683 Wang, J.: Global linear stability of the 2-D shallow-water equations: An application of the distributive
684 theorem of roots for polynomials in the unit circle. *Mon. Wea. Rev.*, 124, 1301–1310, 1996.

685 Wang, J. and Chern, C.: The warm-core eddy in the northern South China Sea, I. Preliminary
686 observations on the warm-core eddy, *Acta Oceanogr. Taiwan*, 18, 92–103, 1987. (in Chinese with
687 English abstract)

688 Weiss, J.: The dynamics of enstrophy transfer in two dimensional hydrodynamics. *Physica D.*, 48, 273–
689 294, 1991.

690 Williamson, G.: Hydrography and weather of the Hong Kong fishing ground. *Hong Kong Fisheries*
691 *Bulletin*, 1, 43–49, 1970.

692 Wu, C. and Chiang, T.: Mesoscale eddies in the northern South China Sea. *Deep-Sea Res. II*, 54, 1575–
693 1588, 2007.

694 Wu, C., Shaw, P. and Chao, S.: Assimilating altimetric data into a South China Sea model. *J. Geophys.*
695 *Res.*, 104(C12), 29987–30005, 1999.

696 Wu, C., Chang, Y., Oey, L., et al.: Air-sea interaction between tropical cyclone Nari and Kuroshio.
697 *Geophys. Res. Lett.*, 35(12), L12605, 2008.

698 Wyrki, K.: Scientific results of marine investigation of the South China Sea and Gulf of Thailand. *Naga*
699 *Rep.* 2, 195, 1961.

700 Xiu, P., Chai, F., Shi, L., Xue, H. and Chao, Y.: A census of eddy activities in the South China Sea during
701 1993–2007. *J. Geophys. Res.*, 115, C03012, doi:10.1029/2009JC005657, 2010.

702 Zhang, F., Wang, W., Huang, Q., Li, Y. and Chau, K.: Summary current structure in Bashi Channel. In
703 Proceedings of Symposium of Marine Sciences in Taiwan Strait and Its Adjacent Waters, 65–72, China
704 Ocean Press, Beijing, 1995.

705 Zhang, Z., Zhao, W., Tian, J. and Liang, X.: A mesoscale eddy pair southwest of Taiwan and its influence
706 on deep circulation, *J. Geophys. Res. Oceans*, 118, 6479–6494, doi:10.1002/2013JC008994, 2013.

707 Zhuang, W., Xie, S., Wang, D., Taguchi, B., Aiki, H. and Sasaki H.: Intraseasonal variability in sea
708 surface height over the South China Sea, *J. Geophys. Res.*, 115, C04010, doi:10.1029/2009JC005647,
709 2010.

710

711

712

713

714

715

716

717

718

719

720

721

722

723

724

725

726

727

728

729

730

731

732

733

734

735

736

737

738

739

740

741

742
743
744
745
746
747

Table 1 Eddy Numbers of different datatype

	AVISO			MO			SCSOFS		
	CYCL	ACYCL	TOTAL	CYCL	ACYCL	TOTAL	CYCL	ACYCL	TOTAL
Spring	6	3	9	6	7	13	6	3	9
Summer	2	3	5	4	7	11	3	5	8
Fall	2	1	3	6	7	13	2	1	3
Winter	5	2	7	5	5	10	1	3	4
Overall	15	9	24	21	26	47	12	12	24

748

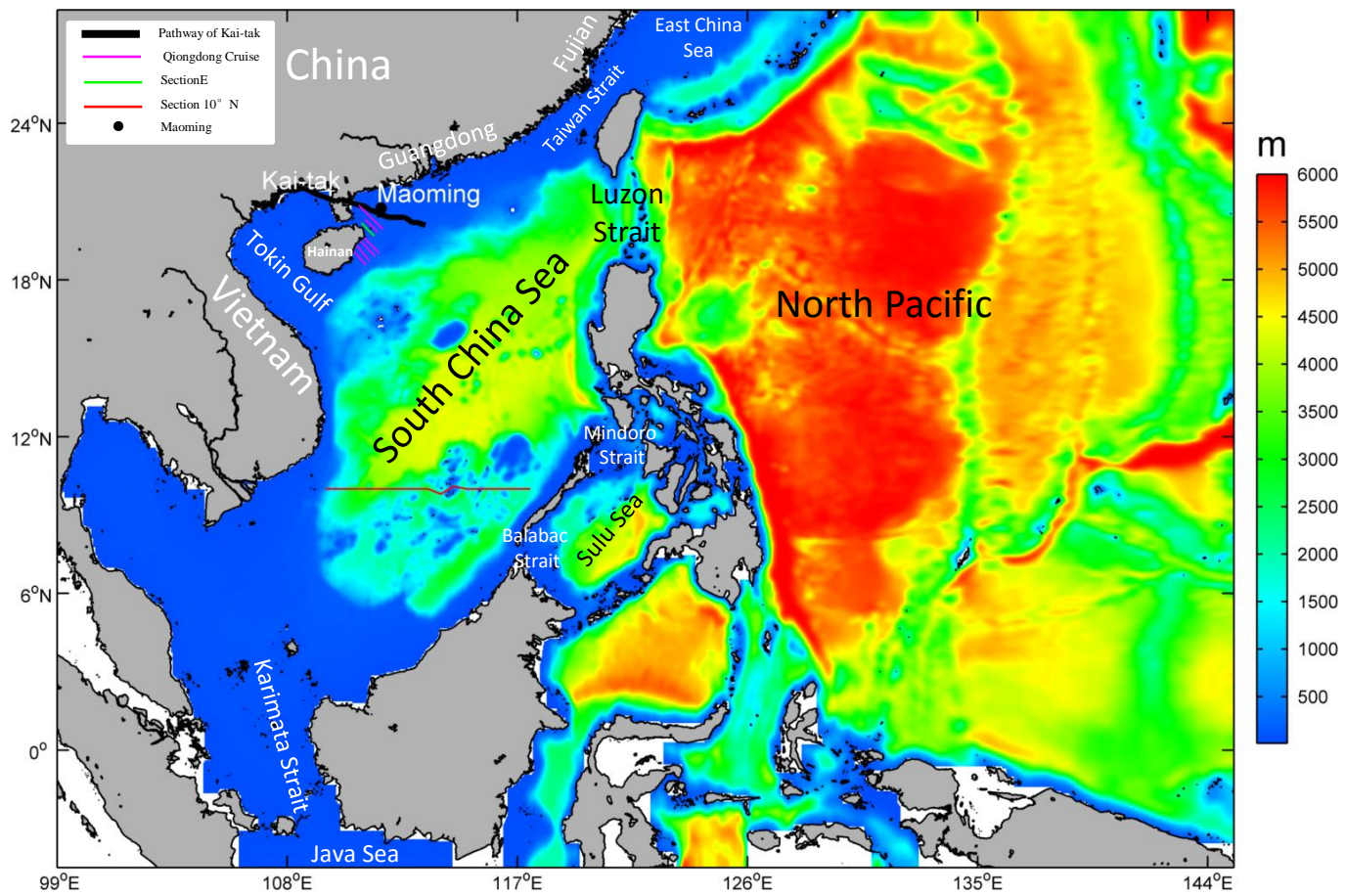


Figure 1: The model domain and bathymetry of SCSOFS.

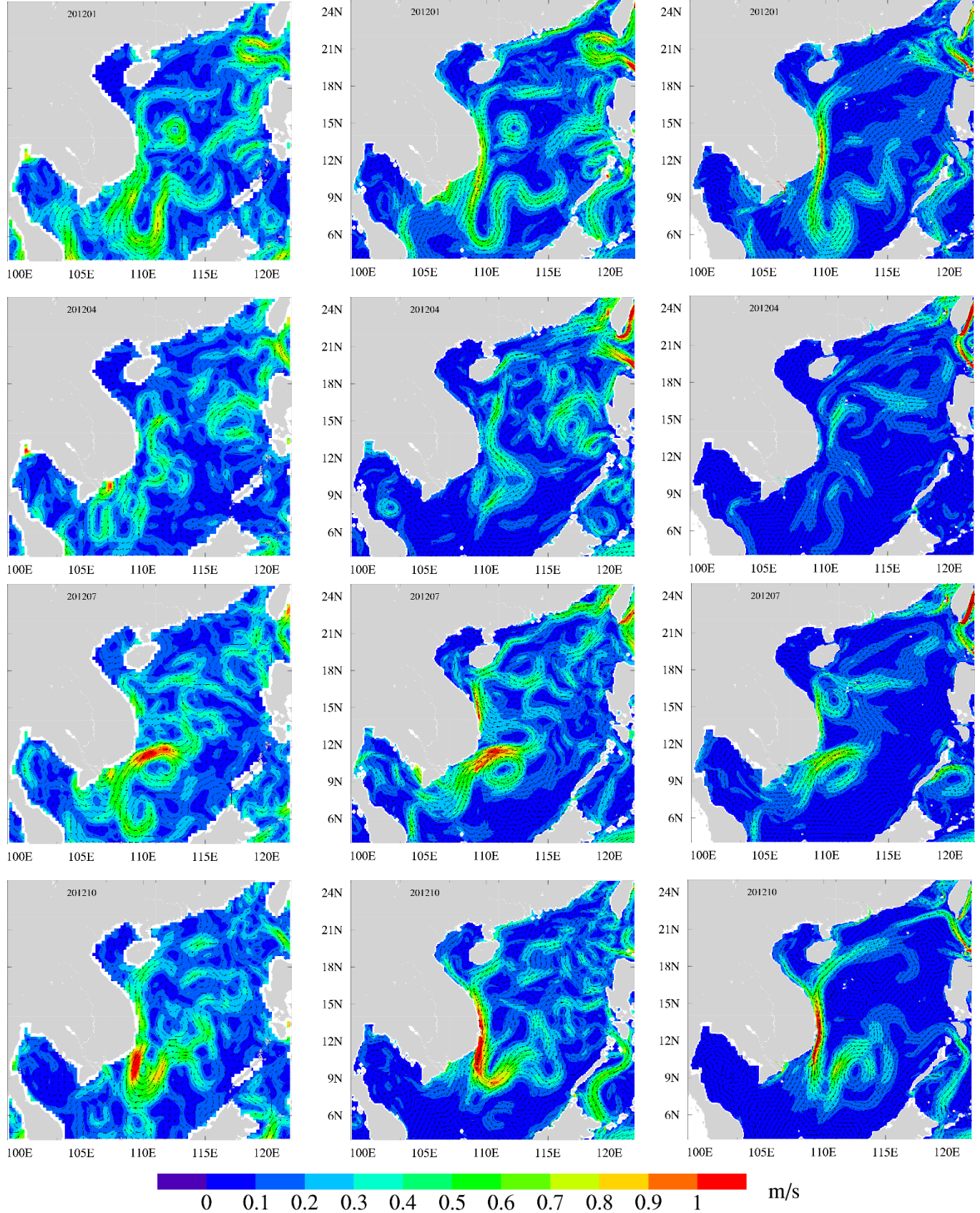


Figure 2: The monthly mean sea surface absolute geostrophic velocity (units: m s^{-1}) in January, April, July, and October, 2012. The left panels are from AVISO, the middle panels are from Mercator Océan, the right panels are from SCSOFS.

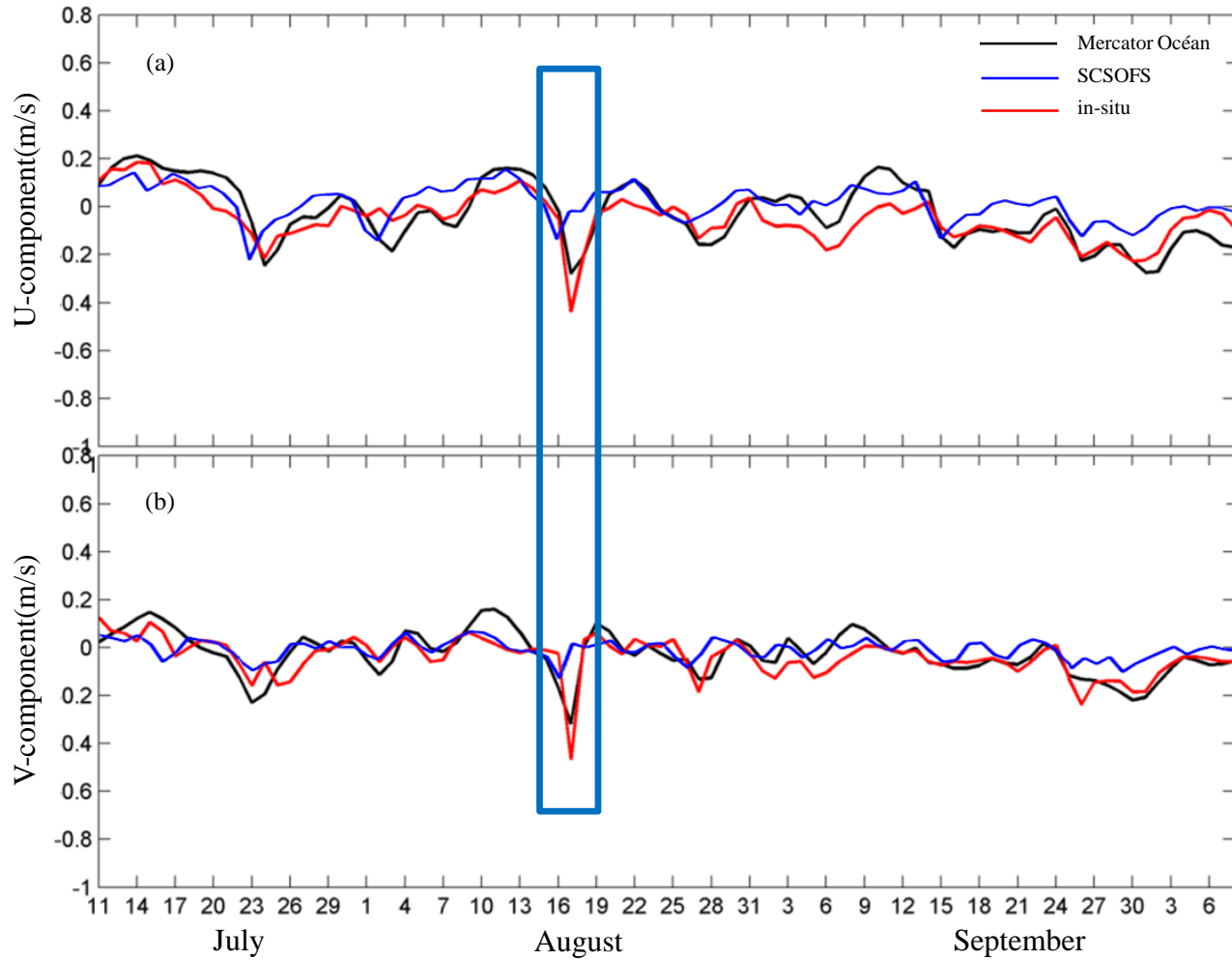


Figure 3: The daily mean time series of u (a) and v (b) components in 40m-depth layer at the Maoming mooring station, from in-situ, Mercator Océan, and SCSOFS.

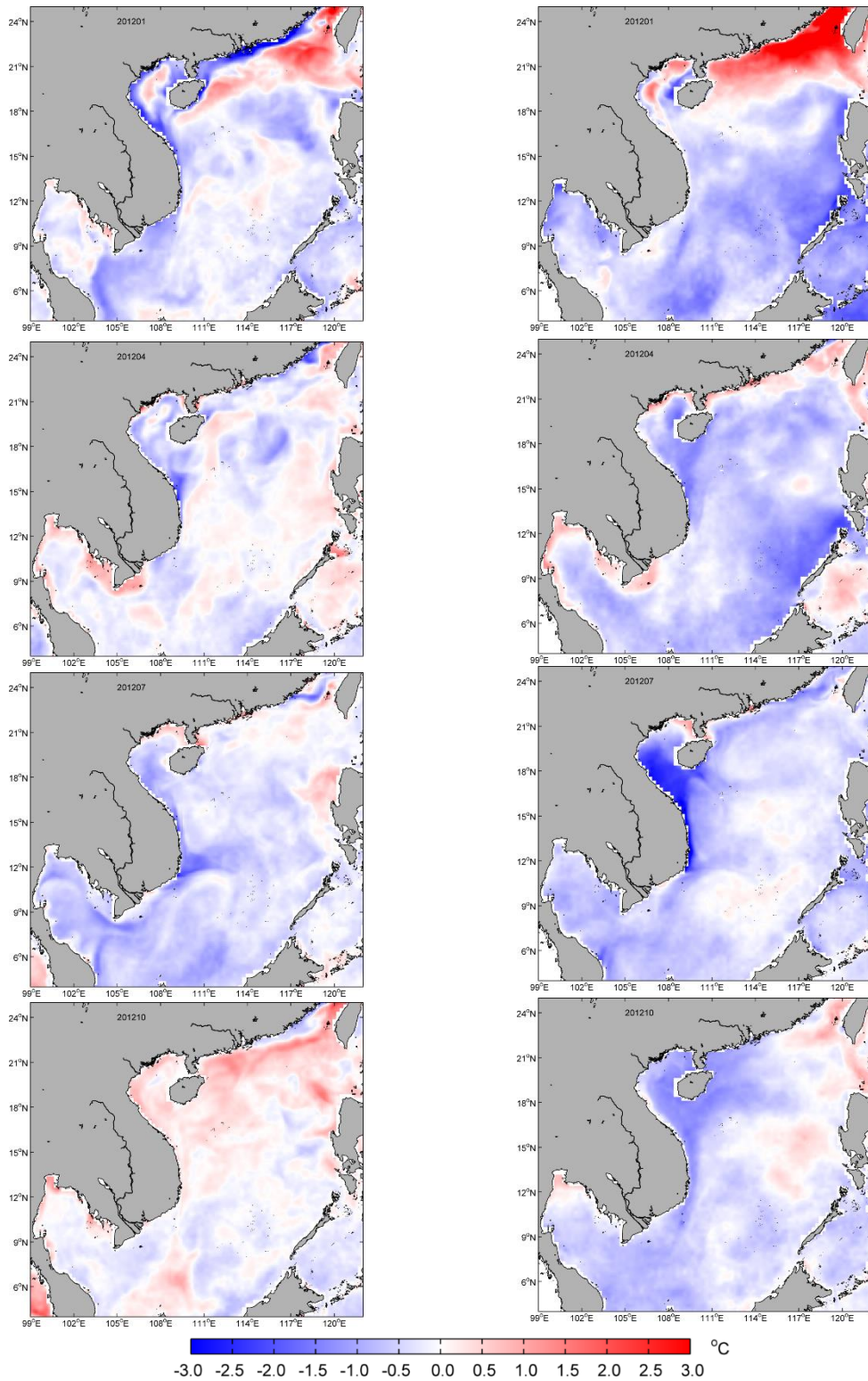


Figure 4: The monthly mean SST error between Mercator Océan (left panels), SCSOFS (right panels) and MGDSSST in January, April, July, and October, 2012

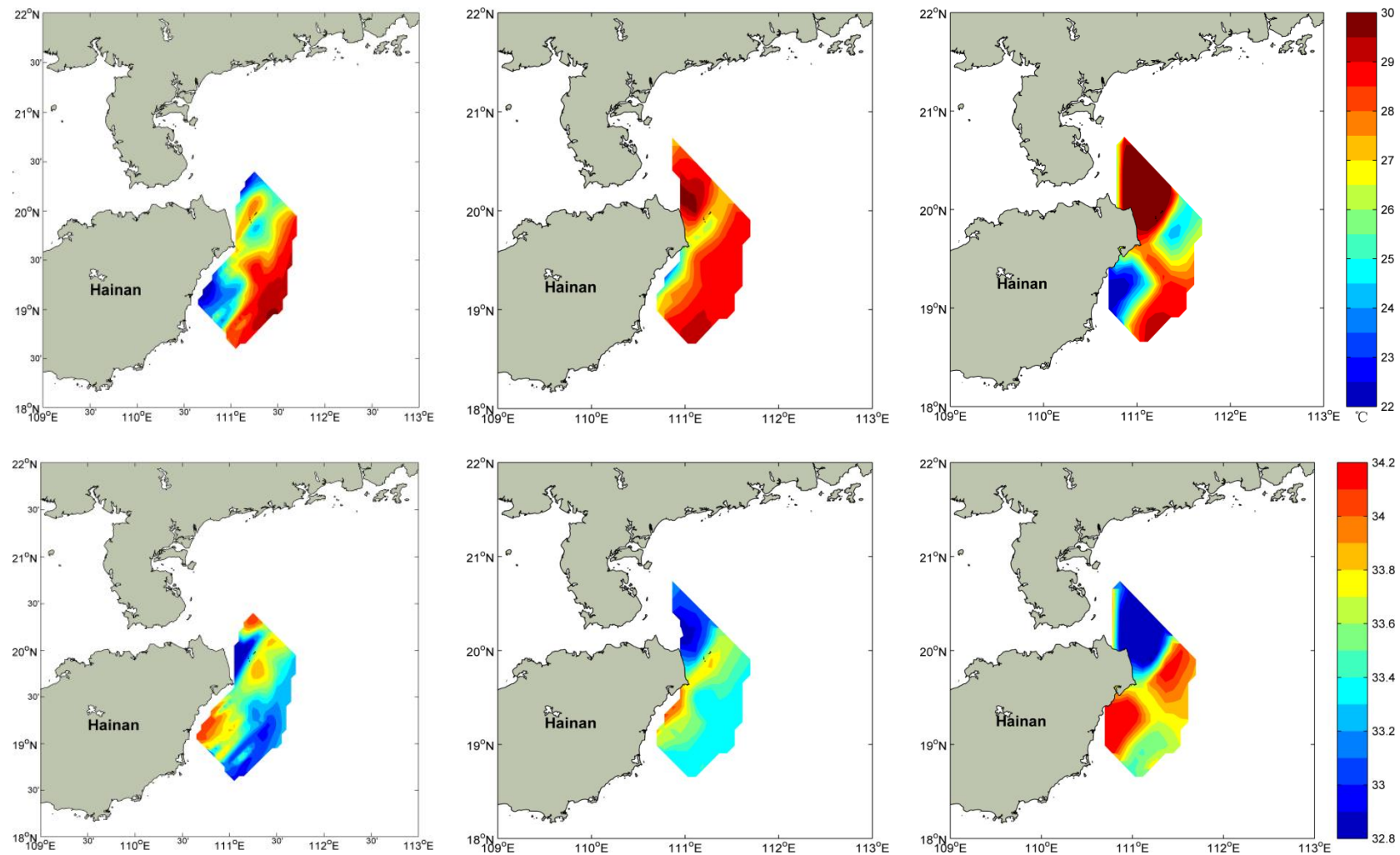


Figure 5: The horizontal distributions of temperature (upper panels) and salinity (lower panels) at 10-m depth layer from the *in-situ* observations of Qiongdong cruise (left column), Mercator Océan (middle column), and SCSOFS (right column), respectively.

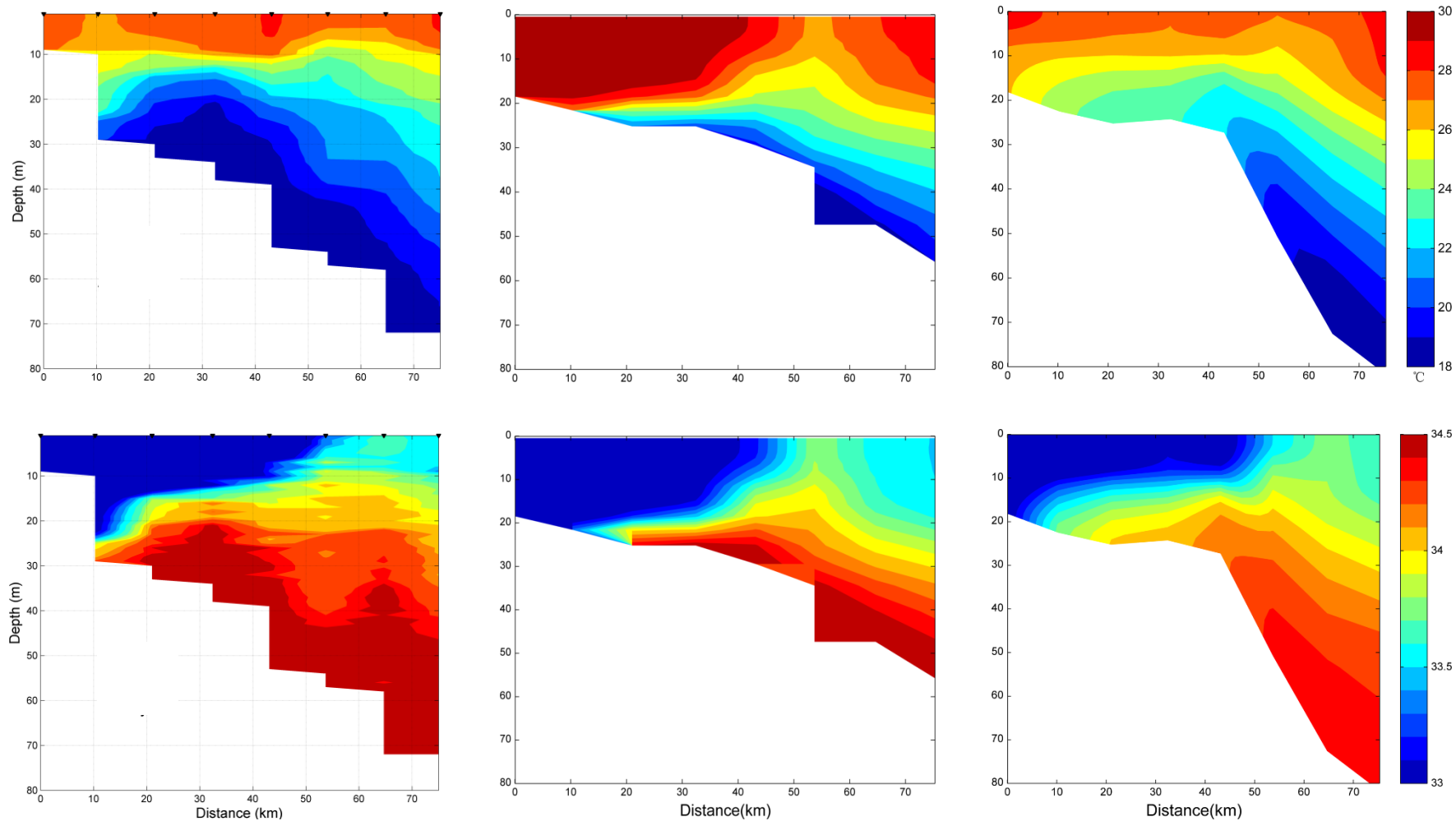


Figure 6: The vertical distributions of temperature (upper panels) and salinity (lower panels) along the section E (See Fig.1) from the *in-situ* observations of Qiongdong cruise (left column), Mercator Océan (middle column), and SCSOFS (right column), respectively.

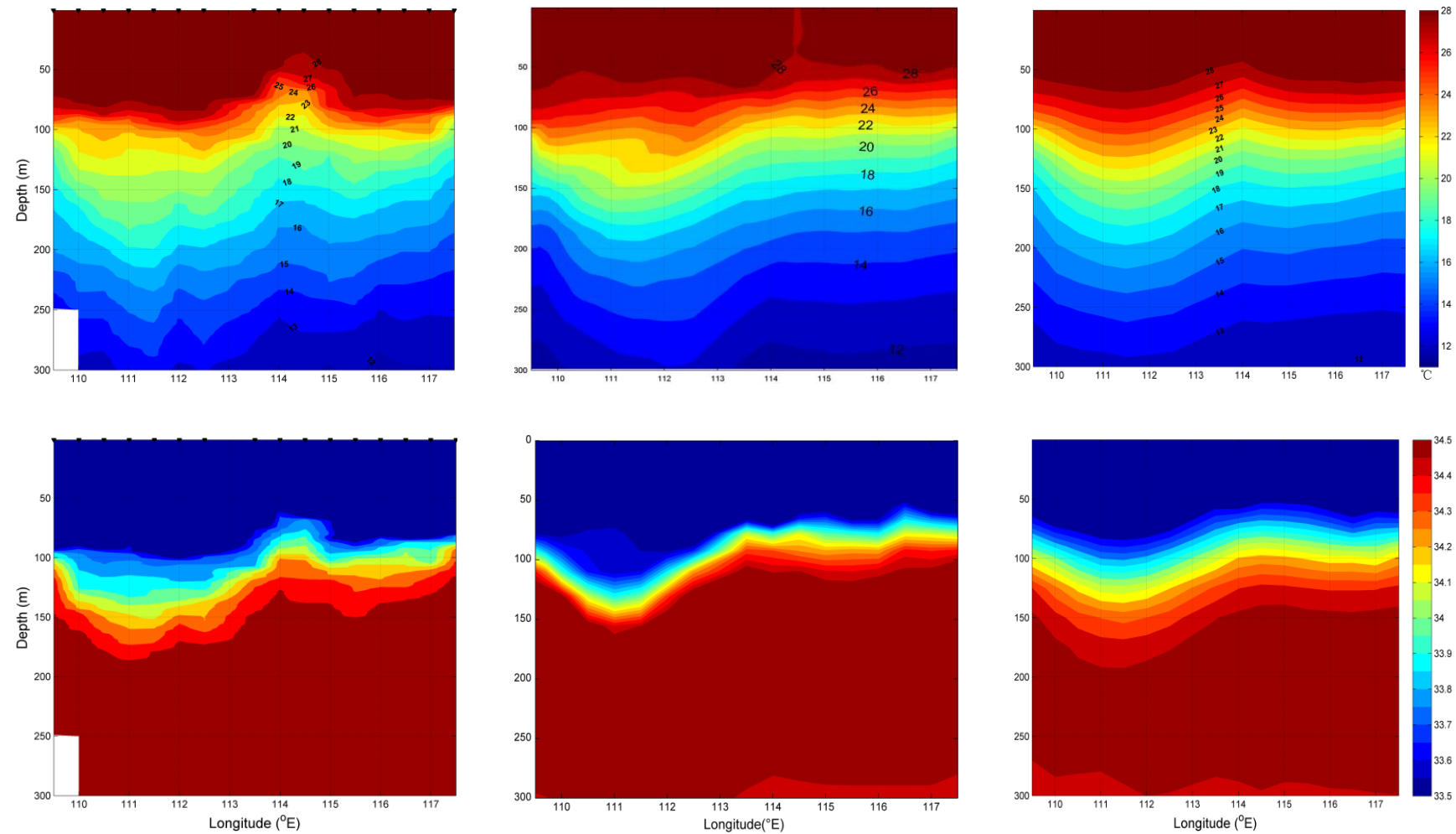


Figure 7: The vertical distributions of temperature (upper panels) and salinity (lower panels) in above 300m depth along the section 10° N from the *in-situ* observations of Nansha cruise (left column), Mercator Océan (middle column), and SCOSFS (right column), respectively.

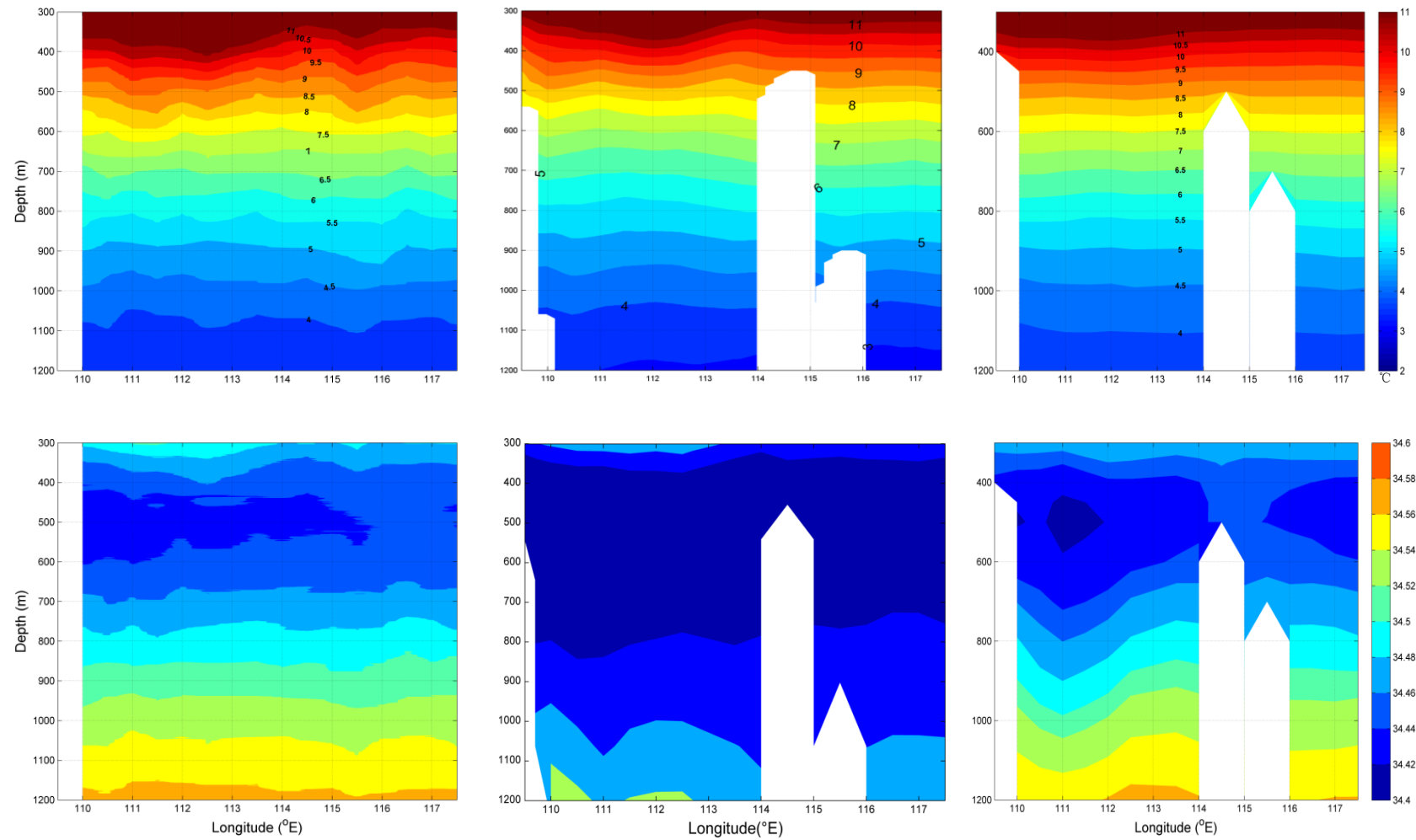


Figure 8: The same with Fig.7, but for the deep layer with depth from 300m to 1200m.

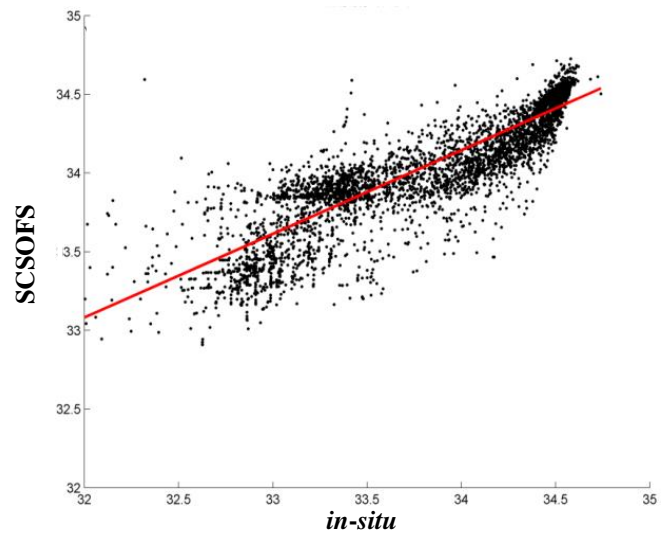
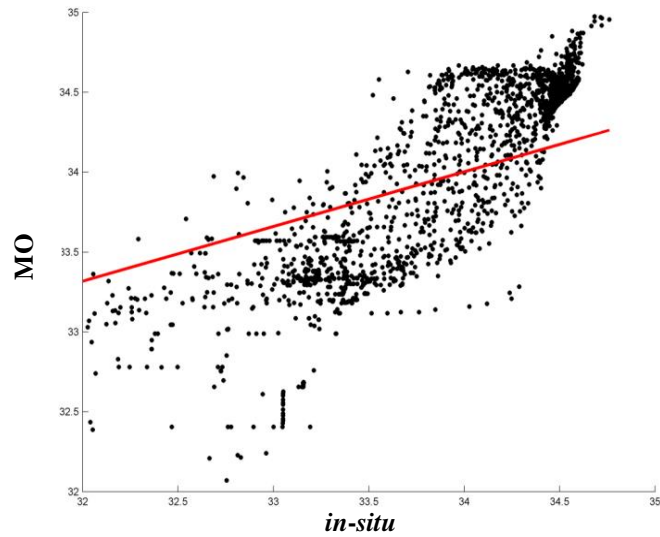
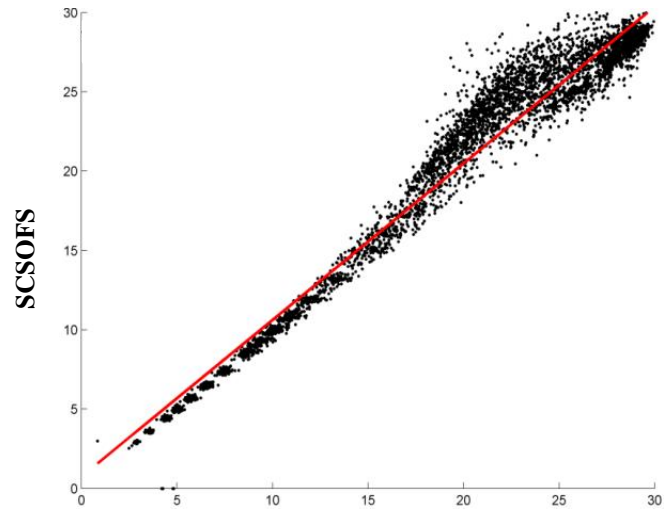
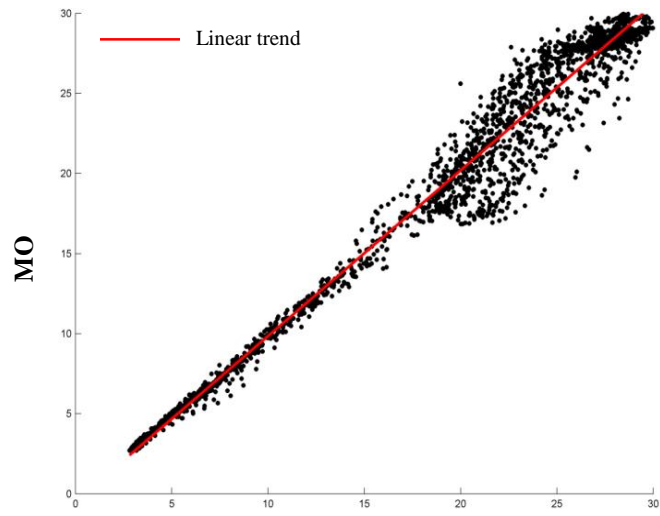


Figure 9: The relative relationships of temperature (upper panels) and salinity (lower panels) between Mercator Océan (left column), SCSOFS (right column) and the *in-situ* observations of all cruises.

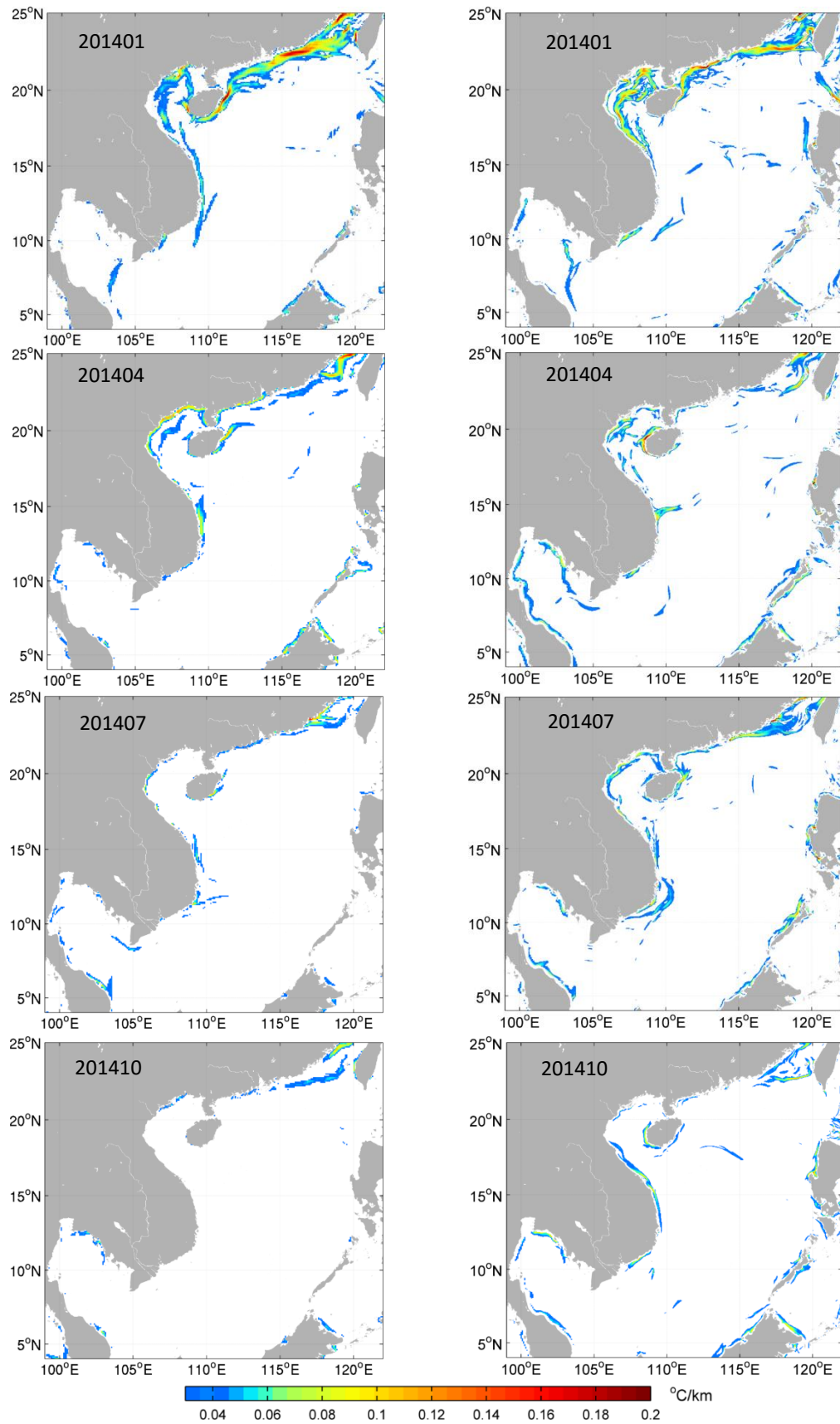


Figure 10: The distributions of SST fronts in the SCS from Mercator Océan (left panels) and SCSOFS (right panels) in January, April, July, and October.

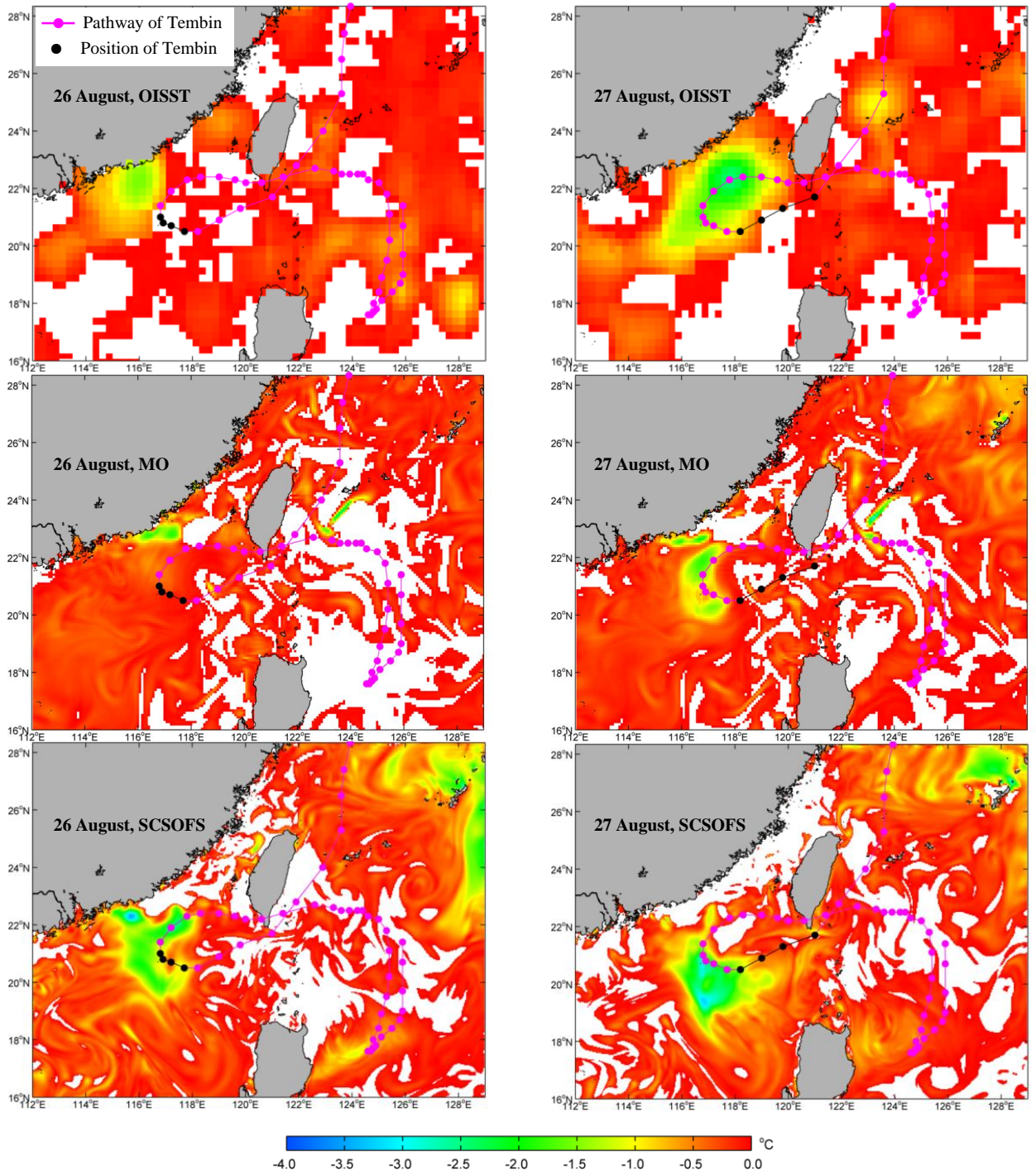


Figure 11: The SST differences of the day from the last day during the period of Typhoon Tembin. The black dots are the positions of the Typhoon Tembin at 00h, 06h, 12h, and 18h on each day.

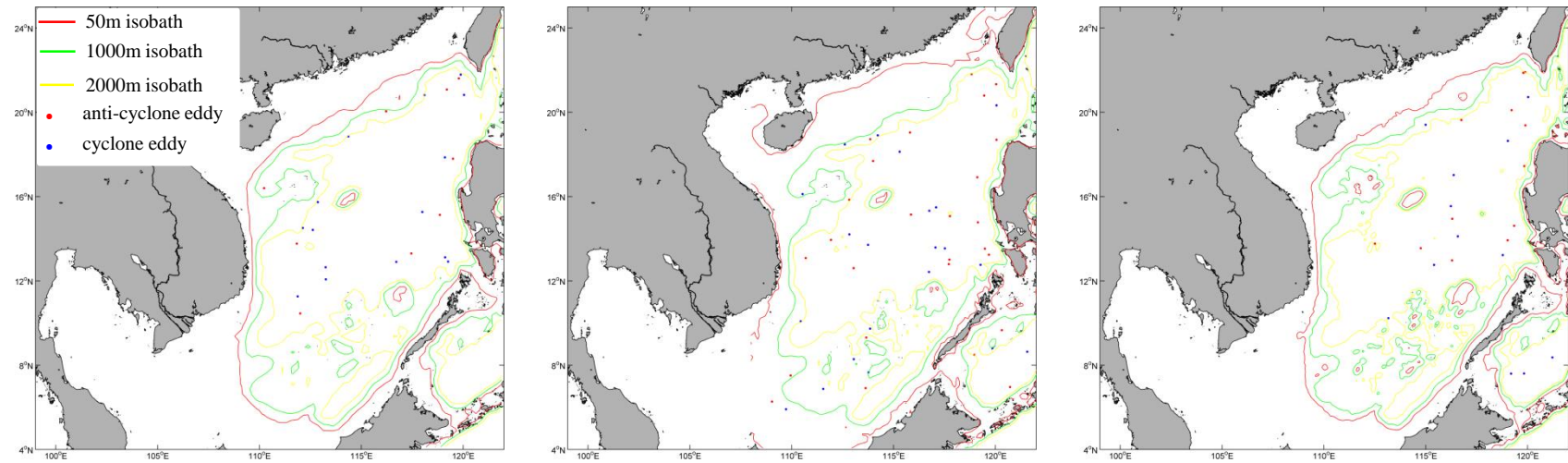


Figure 12: The spatial distributions of eddy birthplace identified using the method of Chaigneau et al. (2008) in the SCS from AVISO (left), Mercator Océan (middle) and SCSOFS (right) in 2012.